The most widespread phage in animals:

Genomics and taxonomic classification of Phage WO

Sarah R. Bordenstein*[1,2] and Seth R. Bordenstein[1,2,3,4]

[1] Department of Biological Sciences, Vanderbilt University, Nashville, Tennessee, USA

[2] Vanderbilt Microbiome Innovation Center, Vanderbilt University, Nashville, Tennessee, USA

[3] Department of Pathology, Microbiology and Immunology, Vanderbilt University, Nashville, Tennessee, USA

[4] Vanderbilt Institute of Infection, Immunology, and Inflammation, Vanderbilt University, Nashville, Tennessee, USA

* Corresponding Author:

Sarah R. Bordenstein, Department of Biological Sciences, Vanderbilt University, Nashville, Tennessee, USA, 615-343-2647, sarah.bordenstein@vanderbilt.edu

Abstract

Wolbachia are the most common obligate, intracellular bacteria in animals. They exist worldwide in arthropod and nematode hosts in which they commonly act as reproductive parasites or mutualists, respectively. Bacteriophage WO, the largest of *Wolbachia*'s mobile elements, includes reproductive parasitism genes, serves as a hotspot for genetic divergence and genomic rearrangement of the bacterial chromosome, and uniquely encodes a Eukaryotic Association Module with eukaryotic-like genes and an ensemble of putative host interaction genes. Despite WO's relevance to genome evolution, selfish genetics, and symbiotic applications, relatively little is known about its origin, host range, diversification, and taxonomic classification. Here we analyze the most comprehensive set of 150 *Wolbachia* and phage WO assemblies to provide a framework for discretely organizing and naming integrated phage WO genomes. We demonstrate that WO is principally in arthropod *Wolbachia* with relatives in diverse endosymbionts and metagenomes, organized into four variants related by gene synteny, often oriented opposite the origin of replication in the *Wolbachia* chromosome, and the large serine recombinase is an ideal typing tool to assign taxonomic classification of the four variants. We identify a novel, putative lytic cassette and WO's association with a conserved eleven gene island, termed Undecim Cluster, that is enriched with virulence-like genes. Finally, we evaluate WO-like Islands in the *Wolbachia* genome and discuss a new model in which Octomom, a notable WO-like Island, arose from a split with WO. Together, these findings establish the first comprehensive Linnaean taxonomic classification of endosymbiont phages that includes distinguishable genera of phage WO, a family of non-*Wolbachia* phages from aquatic environments, and an order that captures the collective relatedness of these viruses.

Introduction

Intracellular, endosymbiotic bacteria comprise some of the most intimate and enduring host-microbe interactions. While reductive evolutionary forces are often presumed to lead to streamlined, tiny genomes, many endosymbionts that host switch contain notable levels of active or relic mobile DNA [1]. An exemplar is the genus *Wolbachia* which harbor transposons [2], temperate phages [3, 4], and putative plasmids [5, 6]. *Wolbachia* are members of the Anaplasmataceae family [7] that also includes the intracellular genera *Anaplasma, Ehrlichia, Neorickettsia, Aegptianella*, and several newly classified bacteria. *Wolbachia* occur in a vast number of invertebrates spanning some nematodes and roughly half of all arthropod species, thus making them the most widespread endosymbionts in animals [8]; but unlike its sister genera, it does not naturally occur in mammalian hosts [9]. Transmission routes are predominantly vertical through the germline, and horizontal transmission of *Wolbachia* in arthropods is frequent on an evolutionary timescale [10, 11], leading to coinfections and subsequent bacteriophage exchanges in the same host [12-16]. Integrated within the bacterial chromosome, these bacteriophages are hot spots of genetic divergence between *Wolbachia* strains [6, 17-20].

Many arthropod-associated *Wolbachia* cause various forms of reproductive parasitism including feminization, parthenogenesis, male killing, and cytoplasmic incompatibility (CI). These selfish modifications hijack sex determination, sex ratios, gametogenesis, and/or embryonic viability to enhance the spread of *Wolbachia* through the transmitting matriline [21, 22]. Nematode-associated *Wolbachia*, however, generally lack phage WO and more often act as mutualists within their animal host [23, 24]. Thus, phage WO was originally hypothesized to contribute to these reproductive manipulations in arthropods through horizontal acquisition and differential

67 expression of parasitism genes that are not part of the core *Wolbachia* genome [20, 23, 25-28].
68 Indeed, transgenic expression of two genes from phage WO or WO-like Islands (genomic islands
69 that are associated with and/or derived from phage WO) demonstrated cytoplasmic incompatibility
70 factors *cifA* and *cifB* as the primary cause of *Wolbachia*-induced CI and rescue [29-32]. In addition,
71 transgenic expression of the WO-mediated killing gene *wmk* recapitulates male-specific embryo
72 lethality and is a candidate for male killing [33]. Conversely, lytic activity of phage WO associates
73 with reduced *Wolbachia* densities and CI levels [34].
74
75 First observed in 1978 as "virus-like bodies" within the gonads of *Culex pipiens* mosquitoes [35],
76 phage WO is a temperate phage that exists in a lysogenic state (the integrated form of a phage
77 genome is termed a prophage) until an event triggers particle production and subsequent lysis of
78 the cell [4, 34, 36-38]. Unlike phages of free-living bacteria, however, the phage particles of
79 intracellular *Wolbachia* contend with a two-fold cell challenge of bacterial and eukaryotic-derived
80 membranes surrounding *Wolbachia* as well as the cytoplasmic and/or extracellular environments
81 of the eukaryotic host. These unique challenges encountered by phage WO presumably selected
82 for the evolution of a novel Eukaryotic Association Module (EAM) that comprises up to 60% of
83 its genome with genes that are eukaryotic-like in function and/or origin [39]. The phage WO
84 genome also features one of the longest genes ever identified in a phage and an abundance of
85 ankyrin repeat domain genes [20, 23, 34, 40, 41], though their function has not been clearly
86 elucidated as it has for the Ankyphages of sponge symbionts that aid in the evasion of the
87 eukaryotic immune system [42]. Given the abundance and importance of phage WO in *Wolbachia*
88 and for understanding genomic flux in endosymbioses worldwide, a firm grasp of its biology,

including classification, evolution, and functions, will be important for establishing and comparing the rules across systems of endosymbiotic phages.

Here we survey prophage WO from 150 *Wolbachia* genome assemblies currently available in the NCBI database [43]. We report the patterns of distribution, chromosomal location, and functions of WO, and we propose a Linnaean classification system according to consultation with the International Committee and their guidelines on Taxonomy of Viruses (ICTV) [44, 45] in which there are three distinguishable phage WO genera within a new taxonomic order encompassing prophages of obligate, intracellular bacteria. We show that WO generally occurs in arthropod-associated *Wolbachia,* and prophage insertions are enriched away from the origin of replication in the bacterial chromosome. We fully annotate the EAM boundaries of representative WO genomes and highlight the presence of the CI genes, *cifA* and *cifB,* and a conserved set of eleven genes, defined here as the *Undecim Cluster*. We also establish a new model suggesting Octomom is derived from the EAM of prophage WO, with implications for Octomom-based pathogenicity, and we determine that all intact prophage WO genomes have a putatively novel patatin-based lytic cassette immediately upstream from the tail module. Finally, we report for the first time, to our knowledge, that prophage WO-like variants occur in diverse bacterial endosymbionts as well as metagenomes of putative symbionts from aquatic environments, providing a deeper understanding of WO origins, evolution, and ecology within and between endosymbiotic bacteria.

Results

Comprehensive survey of *Wolbachia*'s prophage WO and WO-like Islands

Prophage WO elements generally occur in arthropod-associated *Wolbachia*

Wolbachia occur in many protosome animal species of the superphylum Ecdysozoa, while prophage WO has previously been described as restricted to arthropod-associated strains. Because WO molecular surveys typically use single gene markers [15, 16], we comprehensively explored the NCBI database for prevalence of prophage WO, as determined by presence of one or more core phage WO genes (Fig 1a), throughout all sequenced *Wolbachia* genomes. All *Wolbachia* strains are indicated by a lower-case *w* followed by descriptor of host species, and prophage WO genomes are indicated by a WO prefix followed by the same host descriptor (listed in S1 Table).

Fig 1. Prophage WO is modular in structure and associated with all arthropod-infecting *Wolbachia*. (a) A genomic map of prophage WOMelB from the *D. melanogaster w*Mel *Wolbachia* strain highlights phage WO core genes in blue and EAM genes in gray. Genes are illustrated as arrows and direction correlates with forward/reverse strand. The phage WO core consists of recombinase (green), connector/baseplate (royal blue), head (purple), replication and repair (light blue), tail fiber (light pink), tail (salmon), and lysis (brown). The WOMelB EAM encodes *cifA* and *cifB* (cotton candy pink), WO-PC2 containing HTH_XRE transcriptional regulators (lavender), and a conserved set of genes termed the *Undecim Cluster* (navy blue). (b) At least one phage WO core gene (teal) is associated with all sequenced arthropod-*Wolbachia* Supergroups and Supergroup F, which infects both arthropods (blue) and nematodes (purple). The Undecim Cluster (navy blue) is found in the majority of Supergroup A, B, E, and M *Wolbachia* genomes, and CI genes (pink) are encoded by the majority of Supergroup A, B, T, and F genomes. Phage WO elements are absent from all strictly-nematode *Wolbachia* Supergroups. The number of genomes analyzed

is listed in parentheses above each Supergroup. Each bar indicates the % of genomes containing each phage WO element. Source data is provided in S1 Table.

Out of 150 assemblies across nematode and arthropod *Wolbachia*, phage WO occurs in arthropod *Wolbachia* with one exception from the mixed host supergroup of F *Wolbachia* (Fig 1b; S1 Table). All arthropod-associated strains contained evidence of intact or relic phage WO, termed WO-like Islands, and the single instance of WO genes in a nematode occurs in strain *w*Mhie from *Madathamugadia hiepei*, a parasite of the insectivorous South African gecko. The *w*Mhie genome encodes four genes that are conserved throughout phage WO's transcriptional regulation and replication/repair modules (S2 Table) and are not part of the core *Wolbachia* genome. Interestingly, *w*Mhie is a member of Supergroup F that occurs in both arthropods and nematodes. Thus, the presence of phage WO genes in this *Wolbachia* genome supports a horizontal transfer of WO from arthropods to nematodes.

In addition to core phage WO genes, we characterized the widespread distribution of two phage WO elements across arthropod *Wolbachia*: (i) the cytoplasmic incompatibility factor genes *cifA* and *cifB* and (ii) Undecim Cluster (Fig 1b). Generally located within phage WO's Eukaryotic Association Module (EAM [39]; Fig 1a) or in WO-like Islands (genomic islands that are associated with and/or derived from phage WO), *cifA* and *cifB* occur in Supergroups A, B, F, and T; the latter two are newly reported here. *Wolbachia* strains *w*Mov and *w*Oc of Supergroup F both encode phylogenetic Type I *cifA* and *cifB* genes, whereas *w*Chem of Supergroup T encodes Type II *cifA* and *cifB* genes (S3 Table; See [29, 46, 47] for a discussion of *cif* Types). Likewise, we identified a highly conserved set of eleven phage WO-associated genes, hereby termed the Undecim Cluster

(Fig 1a, discussed below), that is distributed across most arthropod Supergroups but notably absent from all nematode *Wolbachia* genomes.

Characterizing the prophage WO genome

Prophage WO genomes are comprised of conserved structural modules and a Eukaryotic Association Module

Prophage WO genomes adhere to the "modular theory" of phage evolution [18] and thus contain conserved structural gene modules (See discussion in S1 Text) and a Eukaryotic Association Module (EAM) [39]. To date, the EAM is unique to *Wolbachia*'s phage WO and as such is often overlooked by prophage prediction algorithms during the bacterial genome assembly process. Moreover, WO can markedly vary in gene content and synteny, and whether this variation does or does not sort into discrete genomic variants has not been investigated. Thus, we sought to identify conserved and distinguishing genomic features for a comprehensive nomenclature system for the community to classify phage WO major groupings. We mapped and re-annotated prophage WO regions from fully sequenced *Wolbachia* genomes to include the EAM and, more generally, incorporate updated annotations for each module.

All prophage WO regions were manually curated based on gene content and synteny (Fig 2; S1-S7 Figs) with regards to eight core phage modules (recombinase, replication & repair, head, connector/baseplate, putative tail fiber, tail, putative lysis, and EAM; labeled in Fig 1) and three newly identified and highly conserved gene clusters shown in Fig 2: (i) WO protein cluster 1 (WO-PC1), corresponding to hypothetical proteins WOCauB3_gp2-gp3; (ii) WO protein cluster 2 (WO-

PC2), located within the EAM and corresponding to putative HTH_XRE transcriptional regulators, DUF2466 (formerly RadC), and hypothetical proteins WOMelB_WD0622-WD0626; and (iii) the Undecim Cluster, an eleven-gene region located within the EAM and corresponding to WOMelB_WD0611-WD0621.

Fig 2. Prophage WO variants feature distinguishable module synteny. Prophage WO variants are organized by genome content and synteny of their structural modules. Sr1WO and sr2WO feature a 5'-core prophage WO region (blue) and a 3'-EAM (gray). Sr3WO features an internal core prophage WO region that is flanked by EAM genes and mobile elements (yellow). Sr4WO is only present in *w*Fol and features three genomic regions with multiple prophage segments. WO-like Islands feature small clusters of prophage WO-like genes; they are comprised of singular structural modules and/or subsets of EAM genes. All modules are color coded: green = recombinase; turquoise = WO-PC1; light blue = replication; purple = head; blue = connector/baseplate; light pink = tail fiber; salmon = tail; brown = putative lysis; lavender = WO-PC2; and navy blue = Undecim Cluster. In addition, ankyrins are shown in red; transposable elements are shown in yellow; and *cifA;cifB* are shown in cotton candy pink. Dotted lines represent breaks in the assembly; module organization is estimated based on closely related variants. Sr1WO is highlighted in hot pink; sr2WO is highlighted in green; sr3WO is highlighted in purple; sr4WO is highlighted in blue; WO-like Islands are highlighted in gray.

There are four distinguishable prophage WO variants: sr1WO, sr2WO, sr3WO, and sr4WO

While gene synteny within each core module is generally consistent, the arrangement of modules across prophage genomes is variable and does not correlate with the early organization of *orf7*-based WO clades, WO-A and WO-B [16, 48]. To formally update this classification with a more comprehensive classification system, we identified conserved WO loci and modular synteny

diagnostic of the four WO arrangement groupings that reflect genus-level ranking. Sequence variation in one gene candidate was consistently associated with similar variation in gene content and synteny: the large serine recombinase [18, 49]. Phage-encoded large serine recombinases facilitate integration of the phage genome into specific attachment sites within the bacterial chromosome as well as control the excision, often with the help of an accessory protein, of the prophage genome during the lytic cycle [50]. A BLASTN analysis of the WO serine recombinase gene confirmed that only those associated with comparable WO module arrangement were full-length reciprocal BLAST hits. Phylogenetic analysis of the recombinase peptide sequence also supported four distinct genus-level clades of prophage WO (common names sr1WO, sr2WO, sr3WO, and sr4WO; nomenclature proposed in [49] and based on the "serine recombinase") as well as closely-related recombinases in prophage regions of non-*Wolbachia* endosymbionts, including the *Paramecium* endosymbiont *Holospora obtusa* (Fig 3a). The genomic content, organization, and chromosomal integration of each srWO variant are described below.

Fig 3. Phylogeny of prophage WO's large serine recombinase correlates with module synteny and genomic integration. (a) A phylogenetic tree of prophage WO's recombinase sequence illustrates the utility of this gene as a WO-typing tool to classify prophage WO variants. Four distinct clades correlate with sr1WO-sr4WO genome organization shown in Fig 2. Non-*Wolbachia* sequences represent similar prophages from other bacterial hosts, such as the prophage HOObt1 of *Holospora obtusa*, an endonuclear symbiont of *Paramecium*. The tree was generated by Bayesian analysis of 283 amino acids using the JTT-IG model of evolution. Consensus support values are indicated for each branch. (*) indicates that the prophage regions are highly degraded; while they likely originated from the corresponding prophage group, they are now classified as WO-like Islands (S7 Fig). (b) Prophage WO integration loci are concentrated opposite the origin of replication, *ori*. All *Wolbachia* genomes have been standardized where each dot represents % nucleotide distance calculated by: (nucleotide distance between 5'-WO and *ori* / genome size) * 100.

(†) indicates the genome is not closed/circularized; genomic locations are estimated based on alignment of contigs to a reference genome (obtained from authors in [51, 52]).

sr1WO. The proposed genus-level taxonomic name for sr1WO, described below, is Cautellavirus. Most sr1WO recombinases integrate into *Wolbachia*'s magnesium chelatase gene, as we previously reported [39], with portions of the bacterial gene found flanking either side of the prophage region. Two exceptions are in: (i) closely-related *w*Ri and wAna where the sr1WO prophage has since been rearranged in the *Wolbachia* genome (S1 Fig) with a portion of the magnesium chelatase now associated with each prophage fragment (S8a-b Fig); and (ii) *w*CauB which contains at least two sr1WO prophages, and WOCauB3 has a secondary intergenic attachment site between *sua5* and a hypothetical protein (S8c Fig).

A key characteristic of sr1WOs is the single domain HTH_XRE transcriptional regulators of WO-PC2 (S1 Fig, lavender) that are located at the 3'-end of the prophage region. Because the genes are fused in most other WO prophages, they are sometimes annotated as pseudogenes (i.e., wRi_p006660 and wRi_p006630 of WORiC) in the *Wolbachia* genome; however, conservation across multiple variants suggests they are functional. Sr1WOs also lack the methylase/ParB gene that is associated with all other WO prophages. A few genomes (i.e, WORiC, WOAnaC, WOSuziC) harbor *cifA* and *cifB* genes, though the origin of these genes remains inconclusive due to a downstream, highly-pseudogenized sr3WO recombinase (wRi_p006680) and adjacent transposases. Finally, all members of the sr1WO group have a distinct 5'-core-prophage region followed by an ankyrin-rich 3'-EAM (Fig 2 and S1 Fig).

sr2WO. The proposed genus-level taxonomic name for sr2WO, described below, is Vitrivirus. sr2WO prophages genes are also organized as 5'-core-prophage followed by 3'-EAM (Fig 2 and S2 Fig), yet module synteny is quite distinct from sr1WO: (i) they lack WO-PC1; (ii) the replication, head, and connector/baseplate modules are reversed; (iii) WO-PC2 is located at the juncture between the core-prophage and EAM regions rather than at the terminal 3'-end of the prophage genome; and (iv) *cifA* and *cifB* genes are absent from assembled genomes thus far. The sr2WO recombinase integrates into variable number tandem repeat 105 (VNTR-105) as previously reported [39], a conserved intergenic region used to type closely-related A-*Wolbachia* strains [53]. While flanking, disrupted portions of the magnesium chelatase correlate with prophage boundaries of sr1WO genomes, disrupted VNTR-105 regions likewise flank the complete sr2WO genome, including the eukaryotic-like *secA* [54] EAM of WOHa2.

Sr3WO. The proposed genus-level taxonomic name for sr3WO, described below, is Taiwavirus. Unlike the previous groups, sr3WO appears to lack a conserved integration site. Rather, these variants feature a core prophage region that is flanked on either side by EAM regions, are separated from adjacent *Wolbachia* genes by an enrichment of transposase-encoding insertion sequences (Fig 2, yellow and S4 Table), and are concentrated away from the origin of replication in the bacterial chromosome (Fig 3b). While their function here is unknown, transposable Mu-like phages replicate via replicative transposition in the bacterial chromosome and, much like phage WO, are associated with severe chromosomal rearrangements and disruptions [55]. Under a similar model, sr3WO transposases could mediate prophage replication and movement throughout the *Wolbachia* genome.

Sr3WO core-prophage module synteny generally resembles that of sr2WO, although a subset of variants also encode an eleven-gene module termed the *Undecim Cluster* (S4 Fig and S5 Fig), discussed in detail below. Most importantly, unlike other prophage WO groups, a majority of the sr3WO variants contain at least one *cifA* and *cifB* gene pair, the locus responsible for *Wolbachia*'s cytoplasmic incompatibility phenotype [29, 30, 32, 46, 47].

Sr4WO. The prophage WO group identified strictly in *w*Fol of *Folsomia candida* springtails is tentatively labelled sr4WO. Unlike the above clades, sr4WO will remain unclassified at the genus level due to high variability and rearrangement of the prophage genomes. A formal classification will be evaluated when more genomes are sequenced that support conserved taxonomic characteristics for the clade. Three variants, broken into multiple segments (S6 Fig), loosely resemble the module synteny of sr3WO. WOFol1 is associated with an Undecim Cluster similar to sr3WO, but all variants contain single-domain HTH_XRE genes similar to sr1WO. The sr4WO prophages contain multiple genomic duplications and mobile elements [56]. While they appear to lack *cifA* and *cifB* genes, they are enriched with multiple copies of *ligA* and resolvase. More variants of this group are needed to analyze chromosomal integration.

WO-like Islands

We identified numerous portions of the prophage WO genome that do not contain enough genetic information to be properly classified. Termed WO-like Islands, they are comprised of single core phage modules, such as a baseplate or tail, and/or genes that are typically associated with the prophage WO genome rather than part of the core *Wolbachia* genome (Fig 2 and S7 Fig). Most WO-like Islands are therefore considered "cryptic", "relic", or "defective" prophages, and likely

298 originated from an ancestral prophage WO genome where they have since been domesticated by
299 the bacterial host or are in the process of degradation and elimination from the chromosome. Based
300 on studies in other systems, conserved prophage genes or gene modules that are not part of a
301 complete prophage are likely to provide a fitness advantage to their host [57, 58] and may interact
302 with, even parasitize, fully intact phages within the same bacterial host [59, 60].
303
304 Like sr3WO prophages, WO-like Islands are often flanked by at least one insertion sequence (S4
305 Table) and are commonly associated with CI genes *cifA* and *cifB*. In the unusual case of the *w*Irr
306 WO-like Island, four CI loci, along with multiple transposases, are arranged in a single genomic
307 cluster that is not associated with conserved WO genes (S7 Fig). We tentatively label the region
308 as a WO-like Island because (i) the *cif* genes and adjacent hypothetical proteins are
309 overwhelmingly associated with prophage WO regions and (ii) there is evidence of a highly
310 disrupted prophage genome about 160kb upstream in the *w*Irr chromosome (S4 Fig) that is also
311 enriched with transposases, allowing for the possibility of a prophage WO origin. Such a model
312 for the putative phage WO origin of one highly studied WO-like Island, *w*Mel's Octomom, is
313 discussed in detail below.
314

315 ## Prophage WO is spatially concentrated away from the origin of replication in
316 ## the *Wolbachia* chromosome

317 To comprehensively examine the association of each prophage WO variant with its chromosomal
318 location in *Wolbachia*, we mapped integration sites, determined by the recombinase or the most
319 5'- WO gene, on the chromosome with respect to normalized distance from the putative origin of
320 replication, *ori* [61]. There is a clustering of prophage WO insertion loci, particularly sr3WOs,

opposite the origin of replication (Fig 3b; Chi-square 2-tailed, p=0.0035) that is similar to the localization patterns of temperate phages in *Escherichia, Salmonella,* and Negativicutes [62-65]. WO chromosomal location patterns support a model in which prophage insertions and WO-like Islands may not be tolerated in regions directly surrounding the origin of replication.

Transposable elements may facilitate transposition and domestication of prophage WO regions

In addition to specific chromosomal integration patterns, we next surveyed the relationship between WO and its associated mobile elements. With the exception of WOCauB3, all fully sequenced prophage WO genomes and WO-like Islands contained at least one transposable element beyond the phage recombinase. The diversity of the WO-associated transposable elements by prophage variant is listed in S4 Table and includes (i) transposases of insertion sequence families IS3, IS4, IS5, IS6, IS66, IS110, IS256, IS481, IS630, IS982; (ii) recombination-promotion nuclease (Rpn), which encodes a PD-(D/E)XK nuclease family transposase; and (iii) reverse transcriptase of group II intron origin (RT). WO's transposable elements are associated with the genomic rearrangement (e.g., WORiC), degradation or domestication (e.g., WORiA), and copy number variation (e.g., WORiB) of various prophage genomes. As discussed above, flanking transposases of sr3WO variants may also play a role in replicative transposition similar to phage Mu.

We observed that reverse transcriptases of group II intron origin (RT) are associated with chromosomal rearrangements, insertions, and/or duplications of multiple sr3WO and sr4WO prophages (illustrated in S9 Fig). Likewise, we identified numerous associations of *cifA;B* gene

pairs with RTs of sr3WO variants (including WOPip1, WOVitA4, WOIrr, WOHa1, WORiB, WOAnaB, WOSuziB) and the *w*Irr WO-like Island. Therefore, the association of CI loci with transposable elements – both within and beyond prophage regions – could be indicative of post-integration genomic rearrangement and/or domestication of the genes, as previously discussed [6]. Below we propose a detailed model and evidence for the most intriguing RT-associated genomic rearrangement, the origin of *w*Mel's Octomom from prophage WOMelA to generate a WO-like Island (Fig 4).

Fig 4. Comparative genomics supports a WO:Octomom origin model for *Wolbachia* proliferation in wMelPop. (a) A new model for Octomom origin predicts the initial infection of *w*Mel with a WOMelA phage. After integration, Octomom splits from the WOMelA core prophage region to form a WO-like Island. (b) A genome map of the putative, intact, ancestral WOMelA where Octomom is highlighted in yellow and the extant WOMelA genome in teal illustrates placement of Octomom in the WO EAM. (c-d) An alignment of the WO-PC2 region with closely related prophages shows that half of the conserved module (WD0507-WD0508) is now associated with Octomom and the other half (WD0257-WD0254) remained with WOMelA prophage region. DUF2466 is split across the genomic regions and, when concatenated, shares homology to intact DUF2466 genes of WO-PC2. An IS5 insertion (d) is associated with single-copy Octomom stability in the *w*Mel chromosome. In wMelCS-like genomes, where the flanking RTs are intact (see S10 Fig), Octomom varies in copy number. (e) When Octomom (orange-yellow) and Octomom-like (green, defined by homology to WD0512, WD0513 and WO-PC2 and illustrated in S10 Fig) regions exist in a single copy, either within or outside the corresponding prophage region, *Wolbachia* proliferation is normal, and it is non-pathogenic. (f) If the WO-like Island occurs in multiple copies or is absent from the genome, *Wolbachia* over-proliferate and are pathogenic. (*) Restoring the 1:1 (WO:Octomom) ratio returns the *w*MelPop phenotype back to normal levels. The association of Octomom with pathogenicity (i.e., correlation vs. causation) is still to be determined [66-68]. NCBI accession numbers are listed for each genome; (†) indicates circular genomes are unavailable and genomic locations are putative.

Unique characteristics of prophage WO

The WO-Octomom Model posits that Octomom is derived from the EAM; *Wolbachia* proliferation may be dependent upon a 1:1 ratio of Octomom : prophage WO

Octomom is a cluster of eight genes in the *D. melanogaster w*Mel *Wolbachia* genome that has been described for its resemblance to a bacterial pathogenicity island (see S10 Fig for genome schematic) [69]. Increasing the environmental temperature of flies either containing multiple copies or completely lacking this region results in *Wolbachia* over-proliferation and pathogenicity [67, 68]. Based on our observations of RT-associated genomic rearrangement, we present a new WO-Octomom Model (Fig 4a) with genomic evidence (Fig 4b-d), in which Octomom putatively originated from the EAM of ancestral WOMelA (sr3WO). First, an ancestral phage WOMelA with core phage genes as well as an Octomom-encoding EAM infects *w*Mel and integrates into the bacterial chromosome. Second, Octomom splits from the prophage EAM region, possibly mediated by RTs, to form an independent WO-like Island about 38kb from the extant WOMelA (Fig 4a). This is supported by gene synteny of the WO-PC2 variant that is split between Octomom and WOMelA at the DUF2466 gene (also annotated as *radC*). Notably, by concatenating the two regions at Octomom's WD0507 (5'-DUF2466) and WOMelA's WD0257 (3'-DUF2466), the gene synteny forms a complete WO-PC2 and closely resembles that of related sr3WO prophages (Fig 4b-d).

Furthermore, Octomom homologs of the two-domain HTH_XRE transcriptional regulator (WD0508) are characteristic of sr2WO and sr3WO prophages, and the *mutL* paralog (WD0509)

393 from Octomom is a phage WO-specific allele [70] that is distinct from the chromosomal *mutL*
394 (WD1306). This supports an ancestral WOMelA prophage genome comprised of core structural
395 modules and an Octomom-containing EAM with intact WO-PC2 (Fig 4b). An alternative
396 explanation could be that genes WD0512-WD0514 existed as a pathogenicity island in the
397 *Wolbachia* chromosome prior to WOMelA infection and later acquired adjacent EAM genes from
398 the prophage to form a complete Octomom Island. In this case, we would expect to find at least
399 one other instance of WD0512-WD0514 occurring independent of prophage regions in other
400 *Wolbachia* strains. Instead, the only *Wolbachia* homologs, to date, are associated with the EAMs
401 of WOPip5 and the wSYT (*Wolbachia* of *Drosophila santomea*, *D. yakuba*, and *D. teissieri*,
402 respectively) prophages [6, 19, 71] (S10 Fig).
403
404 An interesting and robust correlation of this WO-Octomom Model is that one copy relative to
405 prophage WO, either within or outside of the prophage region, is always a distinguishing factor of
406 non-pathogenic *Wolbachia* (Fig 4e), while absence *or* multiplication of Octomom are notably
407 associated with *Wolbachia* over-proliferation and pathogenicity (Fig 4f). This has been previously
408 reported in context of the *Wolbachia* chromosome [66, 67], and we make the distinction here of a
409 *prophage* association to enable a more fine-tuned exploration of Octomom biology. For example,
410 the disruption (*w*Mel) or absence of one (*w*SYT) or both (*w*Pip) flanking RTs correlates with a
411 static 1:1 ratio of the Octomom-like region (i.e., containing WD0512-WD0513 and a
412 transcriptional regulation gene) and its corresponding prophage genome (Fig 4e). Conversely, the
413 region is flanked by identical RTs on either side in all *w*Mel clade VI strains, including *w*MelCS
414 and the dynamic *w*MelPop that ranges from 0 to multiple copies of the WO-like Island (Fig 4f;
415 *w*Mel phylogeny presented in [66, 72]). When the 1:1 ratio in clade VI strains is disrupted, possibly

in conjunction with flanking RTs, *Wolbachia* develops a pathogenic relationship with its animal host [66, 72]. The possible association of RTs with Octomom copy number is also notable due to the observed dependence of both RT activity [73, 74] and *w*MelPop pathology [67, 68] on environmental conditions, such as temperature. The direct role of Octomom on host phenotype is a subject of debate [66, 67], and understanding the association of prophage WO with this region, if any, could inform the biology of this unique system. The two phage-derived regions, for example, may share a common regulatory mechanism since the proposed ancestral splitting of Octomom from WOMelA broke a cluster of transcriptional regulators, namely one transcriptional regulator (WD0508) from the other two (WD0254 and WD0255) that would typically form an intact module. Alternatively, a split of Octomom from its associated prophage genome may influence epigenetic modifications via WOMelA's adenine methylase (WD0267; see [66] for a discussion of epigenetic vs. genetic factors).

Undecim Cluster is a unique eleven gene island associated with prophage WO

Another "pathogenicity island" candidate in the *Wolbachia* chromosome is a highly conserved set of genes (WD0611 to WD0621; Fig 5a) defined here as the *Undecim Cluster (Undecim* is Latin for "eleven"). We identify it in the majority of WO-containing *Wolbachia* genomes (Fig 1b), particularly in association with *cifA*- and *cifB*-encoding regions of sr3WO (S4 Fig and S5 Fig) and WO-like Islands (S7 Fig). Unlike sr3WO prophages themselves, however, the Undecim Cluster does not occur more than once per *Wolbachia* genome. Its complete absence from both *w*Pip and *w*Rec suggests that it is not strictly required for *Wolbachia*'s intracellular survival and/or ability to induce cytoplasmic incompatibility. Rather, it may contribute to variation in host-symbiont interactions [18, 48] by encoding a broad spectrum of metabolic functions and transport potential

[75, 76], including cellular exopolysaccharide and/or lipopolysaccharide (LPS) biosynthesis (WD0611-WD0613; WD0620), methylation (WD0613-WD0614; WD0621), production and export of antibiotics and cytotoxic compounds (WD0615-WD0616) and metabolite transport and biosynthesis (WD0617-WD0619) (Fig 5b). It was identified in phage particle genomes from both *w*VitA and *w*CauB [39], indicating that the region may be transferred between *Wolbachia* strains via the phage. In addition, both RNA-SEQ [77] and mass spectrometry data [75] show that the region is highly expressed. Interestingly, ten of the eleven genes were involved in a lateral gene transfer event between *Wolbachia* and the *Rickettsia* endosymbiont of *Ixodes scapularis* (REIS; [17, 76]) with WD0612 to WD0618 sharing 74% nucleotide identity to a region of the Rickettsial plasmid pREIS2 and WD0619 to WD0621 sharing 67% identity to a region of the bacterial chromosome (Fig 5a). We also identified homologs in *Cardinium hertigii* cHgTN10 (CP029619.1; 67% nucleotide identity) and *Phycorickettsia trachydisci* (CP027845.1; 68% nucleotide identity). While not contiguous in *C. hertigii*, adjacent transposases may have facilitated post-integration rearrangement.

Fig 5. The Undecim Cluster contributes a wide range of cellular processes associated with host-symbiont interactions. (a) A genome map illustrates prophage WO's Undecim Cluster. Gene labels UC1 - UC11 correlate with *w*Mel locus tags WD0611-WD0621. Lines under the genes indicate lateral gene transfer events of this region between *Cardinium hertigii* cHgTN10, *Phycorickettisa trachydisci*, and multiple strains of *Rickettsia*, including the *Rickettsia* endosymbiont of *Ixodes* scapularis (REIS) and its plasmid (pREIS2). Nucleotide identity is listed to the right. Dashed lines indicate that the region is not contiguous in the genome. UC1 shares partial homology with a core *Wolbachia* gene, glmU (WD0133) and was either not involved in the transfer event or has since been lost from non-*Wolbachia* genomes. (b) A cellular model illustrates the putative functions associated with this region. Cellular reactions are highlighted in boxes and membrane transporters are drawn as ovals. *Wolbachia* genes are labeled in blue; Undecim Cluster genes are labeled in red. UC3 (WD0613) is a fusion protein with an N-terminal glycosyltransferase and C-

terminal radical SAM domain; therefore, it is listed twice. Reactions in light gray are likely precursors to multiple pathways in glycosylation, exopolysaccharide biosynthesis, cell division, and/or virulence. Light blue is associated with methylation; dark gray is associated with the production and export of antibiotics and cytotoxic compounds; and navy blue is associated with metabolite transport and biosynthesis. The above functions are predicted based on annotation and homology to other systems. Given the contiguous conservation of the Undecim Cluster throughout prophage WO, all functions, including those not captured in this model, are likely interrelated and influence host-symbiont dynamics.

Phage WO putatively harbors a novel lytic cassette

The most direct impact on *Wolbachia* cellular biology is the potential for phage WO to induce cell lysis [34, 78]. The mechanism of phage-induced cell lysis has been well documented and generally involves a three-component lysis system in gram-negative infecting phages: endolysin, holin, and spanins [79]. This genetic system is noticeably absent from prophage WO genomes, and peptidoglycan, the bacterial target of canonical phage endolysins, has never been detected in *Wolbachia* [80]. We therefore hypothesized that WO phages encode an alternative lytic pathway. The top candidate is a putative and novel patatin-based lytic cassette immediately upstream from the tail module [81].

The cassette contains a patatin-like phospholipase A_2, a small holin-like protein, and an ankyrin-repeat protein. A few prophage WO variants (i.e., WOVitA1, WOAuB, WOPip1, WOPip4, and WOPip5) additionally encode an endonuclease of the phospholipase D family. Patatin-like proteins determine virulence in multiple gram-negative bacteria and specifically facilitate disruption of host cell membranes by *Pseudomonas aeruginosa* and *Rickettsia typhi* [82, 83]. They are significantly more common in pathogenic bacteria and symbionts than in non-pathogens,

suggesting a role in host-association [84]. Holins are not easily annotated because they do not share conserved domain sequence homology, yet several lines of evidence suggest the small protein adjacent to patatin is a "holin-like" candidate: it (i) encodes a single N-terminal transmembrane domain with no predicted charge; (ii) features a C-terminal coiled coil motif; (iii) is smaller than 150 amino acid residues; and (iv) has a highly charged C-terminal domain (S11a Fig) [79, 85, 86]. In addition, homologs of this holin-like gene in prophages from bacterial chromosomes other than *Wolbachia* (e.g., a Tara Oceans Prophage and *Holospora* sp.) are directly adjacent to a GH108 lysozyme, further supporting its holin-like potential (S11b and S11c Fig, Fig 6). The third conserved gene in this module, an ankyrin repeat protein with a C-terminal transmembrane domain, may have the potential to impact membrane stability similar to spanins of the traditional phage lysis model; alternatively, they may play a role in evasion of the arthropod-host immune response similar to those in sponge-associated Ankyphages [42]. Together, this module is fairly conserved across tailed WO phages and is a likely candidate in the exit and/or entry of phage particles through *Wolbachia*'s multiple membranes.

Other prophage genes in the *Wolbachia* chromosome are Gene Transfer Agents (GTAs)

In addition to prophage WO, we identified several non-WO prophage genes (S12 Fig) in the majority of *Wolbachia* Supergroups, including those of the filarial nematodes. Similar to the well-studied GTA of *Rhodobacter capsulatus* (RcGTA; [87, 88]), at least six of these genes encode *E. coli* phage HK97-like conserved domains (S5 Table). We also identified GTA terminase genes associated with the *Wolbachia* chromosome. As reported for *Rickettsiales*, the GTA loci are found in multiple locations across the genome rather than organized in an identifiable prophage-like

cluster [89]. To investigate the evolutionary relationship of the GTA genes with their *Wolbachia* host, we performed individual nucleotide alignments and recovered two highly conserved genetic groups that demarcate Supergroup A and B *Wolbachia* (S13 Fig), supporting vertical descent with modification across these major supergroups. While absent from Supergroups J and L of nematodes, they are present across all other *Wolbachia* Supergroups as well as the closely related genera *Candidatus* Mesenet, *Anaplasma, Ehrlichia*, and *Rickettsia* (S12b Fig). These results imply that *Wolbachia*'s GTA genes are vertically inherited, codiverge with their bacterial hosts, and likely functional given their intact sequences. They are, however, distinct from phage WO, not indicative of former WO-infections, and may be lost during genome reduction.

Prophage WO beyond *Wolbachia*

Prophage WO-like variants occur in diverse bacterial endosymbionts and metagenomes

We identified multiple prophage WO-like variants beyond the *Wolbachia* genus that have gene synteny and nucleotide identity to prophage WO structural modules in: (i) endonuclear bacterial symbionts of *Paramecium* (*Holospora obtusa, H. undulata, H. elegans*, and *H. curviuscula*) [90]; (ii) metagenome projects from an advanced water treatment facility [91], the Indian Ocean (*Tara* Oceans circumnavigation expedition [92]), and a marine aquaculture habitat [93]; (iii) *Candidatus* Mesenet longicola, the CI-inducing bacterial endosymbiont of *Brontispa longissima* [94]; and (iv) multiple strains of *Orientia tsutsugamushi* isolated from humans (Fig 6a). While the structural genes closely resembled those of prophage WO, novel genes were identified in the replication/repair and lysis modules (Fig 6a, genes with prophage WO homology are highlighted

in yellow). All non-*Wolbachia* variants except *Candidatus* Mesenet longicola lacked signature *Wolbachia* phage WO genes such as patatin, ankyrin repeats, and the EAM that are putatively or definitively involved in phage-by-arthropod interactions.

Fig 6. WO-like prophage regions are found in endonuclear *Paramecium* endosymbionts, aquatic environments, and other animal-associated bacteria. (a) Genome maps of non-*Wolbachia* prophage regions illustrate similar gene content and synteny to prophage WO. Locus tags are listed in italics above the genes; NCBI contig accession numbers are shown in the right-hand corner of each genome. Dashed lines represent breaks in the assembly whereas small diagonal lines represent a continuation of the genome onto the next line. Genes with nucleotide homology to prophage WO are highlighted in yellow and genes of similar function are similarly color-coded according to the figure legend. *Candidatus* Mesenet longicola is the only genome to feature EAM genes, including *cifA* and *cifB*. Arrows with diagonal stripes represent genes that may be pseudogenized relative to homologs in other prophage genomes. Genome maps for *H. elegans and H. curviuscula* prophages are not shown. (b) WO-like Islands featuring tail and lysis genes share homology with the *Orientia* regions and may represent phage-derived bacteriocins. Predicted physical structures are illustrated to the left of each genome. Images illustrate the isolation source for each prophage: green borders represent protozoa; blue borders represent aquatic environments; gold borders represent animals.

Relative to the full-length genomes recovered from *Holospora*, *Candidatus* Mesenet longicola and the metagenome projects, *Orientia* prophages appeared to be highly degenerate. These regions featured only tail and lysis genes, but the modules are noticeably intact. Some WO-like Islands, such as WOAlbB2, WONo4, and WOMau3 (Fig 6b), also harbor sole tail and lysis modules. The retention of a complete phage structural module in the bacterial chromosome suggests that it has been domesticated and adapted to benefit the host. For example, several studies report phage-derived bacteriocins that consist of tail and lysis genes and target other strains of the same bacterial species [57]. Similarly, an extracellular contractile injection system (eCIS) comprised of phage

559 tail-like proteins specifically targets eukaryotic cells [95]. Overall, the presence of WO-like
560 variants in non-*Wolbachia* genera continue to support phage WO lateral transfer between
561 unrelated, coinfecting symbionts. This is further evident by the presence of the CI genes, *cifA* and
562 *cifB,* in the *O. tsutsugamushi* genome [96], which may represent a derived variant of phage WO
563 from *Wolbachia* that has since been domesticated by its bacterial host. Alternatively, the
564 association of CI genes in a bacterium harboring WO-like variants could be indicative of two other
565 possible origins - either the last common ancestor of the WO and WO-like phages encoded *cifA*
566 and *cifB,* or the loci may have originated in WO-like phages and transferred to *Wolbachia*. For
567 divergent, horizontally transferred elements, it is often not possible in practice to assign a direction
568 of evolution and origin story.
569

570 ## Linnaean classification of phage WO

571

572 Finally, while phage WO is a model organism to study the tripartite association between viruses,
573 endosymbiotic bacteria, and animal hosts, it is not yet recognized by the International Committee
574 on Taxonomy of Viruses (ICTV). Recently, the ICTV Executive Committee implemented a
575 pipeline for the official classification of viruses from metagenomic datasets [45], including those
576 originating from integrated prophage sequences. Through our comparative analysis of prophage
577 WO sequences here with those that have been sequenced from active particles (i.e., WOVitA1 and
578 WOCauB3), we propose a formal phage WO taxonomy (Fig 7) to align with the ICTV Linnaean-
579 based classification code [44]. The correlation between common name and proposed scientific
580 name for each taxonomic rank is listed in Table 1.
581

582 **Fig 7. Comparative genomics supports a new order-level designation for prophage WO classification.**
583 Symbiovirales is proposed as a new taxonomic order of tailed phages within the class *Caudoviricetes*. It contains
584 viruses that primarily infect *Wolbachia* (proposed family Woviridae) and other symbionts (proposed family
585 Holoviridae). Two proposed subfamilies, Kuehnivirinae and Pipivirinae, distinguish the sr1WO/sr2WO and sr3WO
586 clades (Figs 2 and 3, respectively). Three proposed genera of Woviridae include Cautellavirus (sr1WO), Vitrivirus
587 (sr2WO), and Taiwavirus (sr3WO). sr4WO prophages are currently unclassified. Holoviridae contains a single
588 proposed genus, Paramecivirus, that encompasses closely related prophages of *Holospora* and metagenome-
589 assembled genomes (MAGs) from aquatic environments.
590
591 **Table 1.** The correlation between common name and proposed scientific name is listed for each phage WO exemplar
592 variant and taxonomic rank.

WO Exemplar Variant	Taxonomic Rank	Common Name	Proposed Scientific Name
WOCauB3	Species	WOCauB3	*Wolbachia* virus WOCauB3
	Genus	sr1WO	Cautellavirus
	Subfamily	N/A	Kuehnivirinae
	Family	Phage WO	Woviridae
	Order	WO-like viruses	Symbiovirales
WOVitA1	Species	WOVitA1	*Wolbachia* virus WOVitA1
	Genus	sr2WO	Vitrivirus
	Subfamily	N/A	Kuehnivirinae
	Family	Phage WO	Woviridae
	Order	WO-like viruses	Symbiovirales
WOMelB	Species	WOMelB	*Wolbachia* virus WOMelB
	Genus	sr3WO	Taiwavirus
	Subfamily	N/A	Pipivirinae
	Family	Phage WO	Woviridae
	Order	WO-like viruses	Symbiovirales

593
594 We propose that all phage WO and WO-like viruses be classified in existing class *Caudoviricetes*
595 (phylum *Uroviricota;* kingdom *Heunggongvirae;* realm *Duplodnaviria*) for tailed phages based
596 on the presence of a tail module and observed tail-like structure in electron microscopy [34, 78].

We propose the new order Symbiovirales to recognize the association of these viruses with endosymbionts. Two proposed families, Woviridae and Holoviridae, are named after the first bacterial host identified for each family (*Wolbachia* endosymbionts of arthropods and *Holospora* endonuclear symbionts of *Paramecium*, respectively). Modules shared across the proposed Symbiovirales order are recombinase, replication, head, connector/baseplate, tail fiber, tail, and a putative lytic cassette (See Fig 8 for a summary of taxonomic traits).

Fig 8. Linnaean classification of prophage WO-like viruses is supported by taxonomic traits at the order, family, subfamily, and genus level.

(a) Proposed order Symbiovirales encompasses viruses that infect symbiotic bacteria, contain a large serine recombinase for integration and a PAAR gene in the connector/baseplate module, and feature a conserved set of core phage modules. They share nucleotide homology to *Wolbachia*'s prophages. (b) Subfamilies are classified by presence (Woviridae) or absence (Holoviridae) of an EAM and ankyrin repeat containing proteins. Woviridae may utilize patatin for lysis whereas Holoviridae encode a canonical GH108 endolysin. (c) Two proposed subfamilies address the diversity of chromosomal integration patterns and EAM location of prophages within the Woviridae family. (d) Proposed genera are further distinguished by multiple factors including structural module synteny, HTH_XRE domains, and genome composition.

The suggested family Woviridae encompasses all phage WO and prophage WO variants and is distinguishable by the presence of EAM and eukaryotic-like genes, a patatin-like phospholipase, and multiple ankyrin repeat containing proteins (Fig 8). Upon ICTV approval, Woviridae will be split into two subfamilies - Kuehnivirinae and Pipivirinae - named after the first purification of phage WO particles from *Ephestia kuehniella* [37] and *Culex pipiens* [35], respectively.

621 The proposed Kuehnivirinae will encompass two genera for phages that integrate into discrete *att*
622 sites and feature 3'-placement of the prophage EAM. The first suggested genus of this subfamily,
623 Cautellavirus, recognizes the sequenced genomes from *w*CauB phages [37, 38] and encompasses
624 all sr1WO prophages (Fig 7). Cautellavirus core module synteny (replication, head,
625 connector/baseplate) is inverted relative to other members of the proposed Woviridae; the ankyrin
626 located between the tail module and putative lytic cassette is encoded on the opposite strand; and
627 the genome does not contain a methylase/ParB protein (S1 Fig). The second suggested genus of
628 this subfamily, Vitrivirus, recognizes the first fully sequenced genome from phage WOVitA1
629 particles [39] and encompasses all sr2WO prophages (Fig 7). Members of this genus feature
630 discrete integration into the VNTR-105 locus, and the recombinase is adjacent to ankyrin repeats
631 rather than WO-PC1.
632
633 Members of the proposed subfamily Pipivirinae are currently not associated with distinct *att* sites
634 and are often flanked by EAM-like genes and transposases (S4 Table) on both ends of the
635 integrated genome. Pipivirinae contains only one genus, Taiwavirus, named after the first prophage
636 WO sequence fragment from *w*Tai [3, 78]. The proposed genus Taiwavirus will encompasses all
637 sr3WO prophages (Fig 7) and is the most speciose genus of Symbiovirales. Likewise, it also
638 features the greatest number of degraded prophage regions both within and across diverse
639 *Wolbachia*. As more prophages are sequenced, it may be prudent to further classify this clade into
640 subgenera based on presence or absence of the Undecim Cluster (Fig 2).
641
642 Finally, the WO-like prophages of *Candidatus* Mesenet longicola are likely classified as
643 Woviridae due to nucleotide homology of structural genes and the presence of *cifA;B* containing

644 EAM, but complete sequence information (specifically the recombinase and 5'-region beyond the
645 CI loci) is necessary to definitively classify these phages. Likewise, the *w*Fol prophages will
646 remain as *Unclassified* Woviridae until more genomes are sequenced to provide definitive
647 taxonomic characteristics for the sr4WO variants. As more prophage WO genomes are sequenced,
648 we propose using the srWO designation as a "common name" that roughly correlates with genus-
649 level demarcation and referencing srWO when proposing future additions to the Woviridae
650 taxonomy.
651
652 The proposed family Holoviridae includes the WO-like prophages from most non-*Wolbachia*
653 metagenomic sequences and is currently comprised of phages from aquatic endosymbionts. They
654 lack an EAM and ankyrin repeat containing proteins, feature a GH108 hydrolase rather than
655 patatin-like phospholipase in the putative lytic cassette, and encode LexA and YqaJ that are
656 generally absent from *Woviridae* genomes (Fig 6). Due to gene synteny and sequence homology
657 of these prophage genomes, all species are currently classified into a single Paramecivirus genus.
658 The first representatives of this genus were identified in *Holospora* spp., endonuclear symbionts
659 of *Paramecium caudatum* and *P. bursaria* [97].
660
661 In summary, we propose that viruses should be classified as Symbiovirales based on reciprocal
662 BLAST homology and shared gene content with core phage WO. The large serine recombinase
663 can be used as a typing tool (Fig 3a) and intact genomes for inclusion should include (i)
664 recombinase, (ii) replication and repair, (iii) connector/baseplate, (iv) tail fiber, (v) tail, and (vi)
665 lytic modules. Woviridae are delineated by the presence of a eukaryotic association module
666 (EAM), multiple ankyrin repeats, and a patatin-containing lytic module. Holoviridae are

667 characterized by the absence of an EAM, lack of ankyrin repeats, and a GH108-containing lytic
668 module.
669

670 # Discussion

671 The survey of 150 genomes coupled with manual annotations and comparative sequence analyses
672 offers the most comprehensive overview of *Wolbachia* prophage WO genomics, distribution, and
673 classification to date. From these analyses, we propose four major prophage WO variants
674 corresponding with genus-level Linnaean taxonomy and support the creation of a new order
675 Symbiovirales (within the *Caudoviricetes*) containing two distinct families, Woviridae and
676 Holoviridae. Results presented above suggest that tailed, intact prophage WO genomes serve as a
677 proxy for estimating prophage autonomy vs. domestication in the *Wolbachia* genome where
678 multiple "degraded" prophages and WO-like Islands are indicative of prophage WO domestication
679 by the bacterial host. WO regions enriched with transposable elements contribute to genome
680 plasticity of the bacterial chromosome and may play a role in the domestication of these prophages.
681 One such region, Octomom, has a putative WO origin in which a former EAM region is
682 dynamically replicated or eliminated, and is associated with pathogenicity when not in a 1:1 ratio
683 with its ancestral prophage. Finally, while there is currently no transformation system for
684 *Wolbachia*, future applications may take advantage of conserved integration loci associated with
685 each srWO and utilize the serine recombinase to introduce new genetic material into the bacterial
686 chromosome.
687

688 ## Establishment of the prophage WO database

To assist future analyses of prophage WO, a database of genomes discussed in this study is publicly available at https://lab.vanderbilt.edu/bordenstein/phage-wo/. The Prophage WO Database features sequence data, enhanced annotations, and phylogenetic tools to support: (i) identification of prophage WO regions in newly assembled *Wolbachia* genomes; (ii) annotation of the Undecim Cluster, cytoplasmic incompatibility (*cif*) genes, putative EAM genes, WO-PC2, and other WO-associated regions; and (iii) taxonomic classification of prophage WO-like viruses.

Methods

Prophage WO genome maps and chromosomal integration patterns

Prophage WO regions were manually retrieved from sequenced *Wolbachia* genomes in GenBank via BLASTN searches against each individual *Wolbachia* genome in the Nucleotide (NR/NT) and WGS databases [43]. Genomes from WOCauB3, WOVitA1, WOMelB, WOPip5, and WOFol3 were the primary reference genomes used for each search. Because most prophage regions were incomplete and located at the ends of contigs, we selected more complete assemblies for comparative genomics: *w*Ri, *w*Ana, *w*Suzi, *w*VitA, *w*Ha, *w*Mel, *w*Pip, *w*No, *w*Au, *w*Irr, *w*Fol, *w*AlbB, *w*Mau, and the previously described prophage genomes WOKue, WOCauB2, WOCauB3, WOSol, WORecA, and WORecB (See S1 Table for accession numbers). All genomes were reannotated in Geneious Prime v2019.2 using the InterProScan [98] plug-in along with information from BLASTP [99], Pfam [100], HHPRED [101], ISFinder [102], and SMART [103] databases. Prophages were then organized into groups based on similar gene content and module organization. Whole genome alignments were performed with the Mauve [104] plug-in in Geneious.

Prophage genomic boundaries for sr1WO and sr2WO were defined by 5' and 3' homology to a known *attP* site (discussed below). Prophage genomic boundaries for sr3WO and sr4WO were identified by translating each prophage gene and "walking out" from the structural modules by using a BLASTP of each gene product against the core *Wolbachia* genome. If a gene was identified in most *Wolbachia* strains, including those infecting nematodes, as well as in the closely related genera *Ehrlichia* and *Anaplasma,* it was considered a core *Wolbachia* gene and not included in the

718 prophage annotation. If a gene was only present in WO-like regions of other *Wolbachia* genomes,
719 it was considered a phage-associated gene. Because the HTH_XRE transcriptional regulators
720 (WO-PC2) were identified in phage purifications from WOCauB3 and WOVitA1, any genes
721 located between the structural modules and WO-PC2 were considered part of the prophage
722 genome. Through this method, we identified flanking 5' and 3' transposases that separated phage-
723 associated genes and the bacterial chromosome in sr3WO and sr4WO regions. Because some
724 transposable elements did not fall within the known IS Groups for *Wolbachia [2]*, they were
725 comparably annotated to IS Family using ISFinder.
726
727 Chromosomal integration patterns were analyzed by similarly aligning all circular genomes based
728 on the putative origin of replication, *ori* [61]: WD1027 (CBS domain-containing)-like genes were
729 oriented in the reverse direction and WD1028 (*hemE*)-like genes were oriented in the forward
730 direction. The nt-distance from *ori* to the prophage recombinase, or 5'-gene, was divided by the
731 length of the total *Wolbachia* genome and multiplied by 100 for a % distance from *ori*. The *w*VitA
732 and *w*Rec genome arrangements may not be exact as they contain multiple scaffold breaks and
733 genome orientation was estimated based on homology to closely related genomes.
734

735 ## Recombinase homology and phylogenetics

736 Large serine recombinase genes from each reference genome were translated and aligned using
737 the MUSCLE [105] plugin in Geneious. The best model of evolution, according to corrected
738 Akaike information criteria, was determined by ProtTest [106, 107] and the phylogenetic tree was
739 constructed using default parameters of the MrBayes [108] plugin in Geneious with Rate

Matrix=jones and Rate Variation=invgamma. A Consensus Tree was built with a support threshold of 50% and burn-in of 10%.

Phage WO *att* sites

The *attP* sites for WOVitA1 and WOCauB3 were previously identified by sequencing active phage particles and confirmed with PCR and Sanger sequencing [39]. Each *attP* sequence was submitted as a BLASTN query against *Wolbachia* genomes harboring similar prophage haplotypes to identify specific *attL* and *attR* sites. The *attB* sites were predicted by concatenating chromosomal sequences adjacent to *attL* and *attR*. The predicted *attB* sites were then used as queries in a BLASTN search against *Wolbachia* genomes to confirm that the sequences exist, uninterrupted, in chromosomes lacking similar prophage haplotypes.

Phage WO beyond *Wolbachia*

Contigs containing WO-like prophage regions in *Holospora*, *Orientia*, *Candidatus* Mesenet, and multiple metagenome-associated taxa were identified by a BLASTP query of prophage WO sequences against the NCBI database. The nucleotide sequence for each homolog (usually a contig in the WGS database) was manually inspected for WO-like regions. If detected, the boundaries of each prophage region were determined using the similar "walk out" BLASTP approach described above, looking for homology to other phage or bacterial genes. All non-Anaplasmataceae prophage genomes had concise boundaries (recombinase and lysis module) that did not include an EAM.

Identification of Gene Transfer Agents

The genome annotations used for comparative genomics were manually inspected for keywords *phage*, *capsid*, and *tail*. Any gene not within an annotated prophage WO region was translated and a BLASTP was performed against the NCBI database. Based on top hits, genes were binned into "WO-like" indicating homology to phage WO and "GTA" indicating homology to HK97 phage.

Taxonomic Classification

The proposed taxonomic classification of phage WO was drafted in accordance with ICTV guidelines for genome-based taxonomy [109] and will be formally reviewed by the Committee in the next cycle. Specifically, it is recommended that phages should be assigned the same species if their genomes are more than 95% identical; assigned the same genus if genomes share 80% nucleotide identity across the genome length and form monophyletic groups based on a phylogenetic tree of signature gene(s); assigned the same subfamily (optional) if they share a low degree of sequence similarity and the genera form a clade in a marker tree phylogeny; assigned the same family if they share orthologous genes and form a cohesive and monophyletic group in a proteome-based clustering tool; and assigned the same order when two or more families are related. Prophage WO taxonomic classification satisfied all demarcation criteria except for genus designation. At the genus level, due to the high variability of the EAM, we applied alternative criteria: genomes should (i) share >70% nucleotide homology across >30% of the genome; (ii) form a distinct phylogenetic clade based on the amino acid sequence of the signature typing gene, large serine recombinase; and (iii) demonstrate shared gene and module synteny.

Supplementary Figures

S1 Fig. Cautellavirus (sr1WO) genome maps. Genome maps of sr1WO prophage regions where genes are drawn to scale in forward and reverse directions. Predicted physical structures are illustrated to the left of each genome. All genomes contain tail modules with the exception of the partial WOVitA2 sequence. Prophage WO Core Genes are shaded in blue and predicted EAM genes are shaded in gray. Genes of similar function are similarly color-coded according to the figure legend. Locus tags, if available, are listed in italics above the genes. The large, black diagonal lines between the recombinase and transposase in WORiC and WOSuziC represent post-integration rearrangement of the prophage region in the *Wolbachia* chromosome. Dashed lines represent breaks in the assembly whereas small diagonal lines represent a continuation of the genome onto the next line. Arrows with diagonal stripes represent genes that may be pseudogenized relative to homologs in other prophage WO genomes. The putative function for each structural gene is discussed in S1 Text.

S2 Fig. Vitrivirus (sr2WO) genome maps. Genome maps of sr2WO prophage regions where genes are drawn to scale in forward and reverse directions. Predicted physical structures are illustrated to the left of each genome. WOVitA1-like prophage genomes encode all structural modules (shaded in blue) and an EAM (shaded in gray) whereas WORiA-like prophage genomes encode an intact head module, recombinase, lysozyme, AAA16, and disrupted connector. They lack most other modules. Genes of similar function are similarly color-coded according to the figure legend. Locus tags, if available, are listed in italics above the genes. Dashed lines represent breaks in the assembly whereas small diagonal lines represent a continuation of the genome onto

808 the next line. Arrows with diagonal stripes represent genes that may be pseudogenized relative to
809 homologs in other prophage WO genomes. The putative function for each structural gene is
810 discussed in S1 Text.
811
812 **S3 Fig. Taiwavirus (sr3WO) genome maps.** Genome maps of sr3WO prophage regions where
813 genes are drawn to scale in forward and reverse directions. Three *w*Pip prophages exist as one
814 contiguous prophage region in the *Wolbachia* genome and are illustrated here as WOPip1,
815 WOPip2, and WOPip3 (based on [110]). Predicted physical structures are illustrated to the left of
816 each genome. Prophage WO Core Genes are shaded in blue and predicted EAM genes are shaded
817 in gray. Genes of similar function are similarly color-coded according to the figure legend. sr3WO
818 is comprised of highly variable genomes that are often flanked by mobile elements (transposases
819 are shown in yellow). They generally contain a recombinase, connector/baseplate, head, and EAM
820 with only a few genomes encoding a complete tail. Prophages in this group often contain *cifA;B*
821 (pink). Locus tags, if available, are listed in italics above the genes. Dashed lines represent breaks
822 in the assembly whereas small diagonal lines represent a continuation of the genome onto the next
823 line. Arrows with diagonal stripes represent genes that may be pseudogenized relative to homologs
824 in other prophage WO genomes. The putative function for each structural gene is discussed in S1
825 Text.
826
827 **S4 Fig. Taiwavirus (sr3WO and sr3WO-Undecim Cluster) genome maps.** Genome maps of
828 sr3WO prophage regions where genes are drawn to scale in forward and reverse directions. WOIrr
829 is one contiguous prophage region in the *Wolbachia* genome that is illustrated here as Segment 1
830 and Segment 2. A subset of sr3WO prophages is further categorized by the presence of a highly

conserved WD0611-WD0621 like region, termed the Undecim Cluster (navy blue). Predicted physical structures are illustrated to the left of each genome. Prophage WO Core Genes are shaded in blue and predicted EAM genes are shaded in gray. Genes of similar function are similarly color-coded according to the figure legend. sr3WO is comprised of highly variable genomes that are often flanked by mobile elements (transposases are shown in yellow). Prophages in this group often contain *cifA;B* (pink). Locus tags, if available, are listed in italics above the genes. Dashed lines represent breaks in the assembly whereas small diagonal lines represent a continuation of the genome onto the next line. Arrows with diagonal stripes represent genes that may be pseudogenized relative to homologs in other prophage WO genomes. The putative function for each structural gene is discussed in S1 Text.

S5 Fig. Taiwavirus (sr3WO-Undecim Cluster) genome maps. Genome maps of sr3WO prophage regions where genes are drawn to scale in forward and reverse directions. This subset of sr3WO prophages is further categorized by the presence of a highly conserved WD0611-WD0621 like region, termed the Undecim Cluster (navy blue). Predicted physical structures are illustrated to the left of each genome. Prophage WO Core Genes are shaded in blue and predicted EAM genes are shaded in gray. Genes of similar function are similarly color-coded according to the figure legend. sr3WO is comprised of highly variable genomes that are often flanked by mobile elements (transposases are shown in yellow). Prophages in this group often contain *cifA;B* (pink). Locus tags, if available, are listed in italics above the genes. Dashed lines represent breaks in the assembly whereas small diagonal lines represent a continuation of the genome onto the next line. Arrows with diagonal stripes represent genes that may be pseudogenized relative to homologs in other prophage WO genomes. The putative function for each structural gene is discussed in S1 Text.

S6 Fig. Unclassified (sr4WO) genome maps. Genome maps of sr4WO prophage regions where genes are drawn to scale in forward and reverse directions. To date, sr4WO prophages have only been identified in the parthenogenic strain of *Folsomia candida*, *w*Fol. WOFol2 is one contiguous prophage region in the *Wolbachia* genome that is illustrated here as Segment 1 and Segment 2. Likewise, the WOFol3 prophage region is illustrated as three segments. Predicted physical structures are illustrated to the left of each genome. Prophage WO Core Genes are shaded in blue and predicted EAM genes are shaded in gray. Genes of similar function are similarly color-coded according to the figure legend. Locus tags, if available, are listed in italics above the genes. Small diagonal lines represent a continuation of the genome onto the next line. Arrows with diagonal stripes represent genes that may be pseudogenized relative to homologs in other prophage WO genomes. The putative function for each structural gene is discussed in S1 Text.

S7 Fig. WO-like Island genome maps. Genome maps of WO-like Islands where genes are drawn to scale in forward and reverse directions. These regions contain only one structural module and/or group of WO-related genes. Regions flanked by assembly breaks (i.e., WORecB, WORecA, and *w*VitA) are tentatively classified as WO-like Islands due to lack of a full-length prophage in the genome assembly. Names are based on the original author's description. If it was identified as a prophage in the genome announcement, the reported WO name is listed here. Otherwise, the name simply refers to the encoding *Wolbachia* genome. Many WO-like Islands contain *cifA;B*; some Islands (i.e., *w*No, *w*VitA, WOMau4, and WOAlbB3) contain both Type III *cifA;B* (pink) and the Undecim Cluster (navy blue). Predicted physical structures are illustrated to the left of each genome. Prophage WO Core Genes are shaded in blue and predicted EAM genes are shaded in

gray. Genes of similar function are similarly color-coded according to the figure legend. Locus tags, if available, are listed in italics above the genes. Dashed lines represent breaks in the assembly. Arrows with diagonal stripes represent genes that may be pseudogenized relative to homologs in other prophage WO genomes. The putative function for each structural gene is discussed in S1 Text.

S8 Fig. *In silico* predictions of phage WO attachment (*att*) sites. An integrated prophage sequence contains left and right attachment sites (*attL* and *attR*, respectively) at the points of chromosomal integration. Half of the *att* site is phage-derived (green); the other half is bacterial derived (black). If the DNA sequence of the bacterial attachment site (*attB*, black) is known, a nucleotide alignment of the intact sequence with the integrated prophage genome will correlate with 5'- (*attL*) and 3'- (*attR*) prophage boundaries. (a) WORiC, a member of sr1WO, integrates into *w*Ri's magnesium chelatase gene. By aligning an intact copy of this gene (WD0721) from closely related *w*Mel that does not harbor sr1WO, (b) the juncture points of the disrupted magnesium chelatase indicate the *attL* and *attR* sites for the WORiC prophage region within the *w*Ri genome. (b) The phage attachment site (*attP*, green) is predicted *in silico* by concatenating the non-*Wolbachia* portions of the *attL* and *attR* sites. (c) Likewise, this method can also be applied when the bacterial integration locus is intergenic. The homologous intergenic region of closely related, sr1WO-free *w*Pip can be used to predict *att* sites for WOCauB3. Nucleotides in orange represent a common region, O, that is shared by all four *att* sites. This method was adapted from [39] where the *attP* site was used to predict the *attB* site of sr2WO phages.

S9 Fig. RT is associated with duplication, inversion, and recombination of the prophage WO genome. (a) The WOMelB prophage genomes of *w*Mel2_a and *w*Mel2_b are duplicated relative to the *w*Mel reference genome [72]. (b) The entire WORiB prophage region is duplicated in *w*Ri [19]. (c) WOHa1 encodes a second, pseudogenized *cifA;B*-containing region relative to closely related WOAuA, WORiB, WOSuziB, and WOSol prophages. (d) A ligase-containing region is duplicated in *w*Fol's WOFol1 and WOFol2 [56]. (e) Based on homology to other prophage regions (Fig 2), the connector/baseplate should be adjacent to a head module and the WOPC-2 and replication genes should be oriented in the opposite direction; this indicates a likely insertion and/or recombination in the WOFol3 prophage region. (f) The WOIrr head module is inverted relative to other sr3WOs. Genes are illustrated as arrows; putative gene annotations are labeled in S1-S7 Figs. In each example, the regions of chromosomal rearrangement are highlighted in light orange and flanked by at least one RT.

S10 Fig. Comparative genomics of Octomom-like variants across diverse *Wolbachia*. Octomom (yellow-orange) and Octomom-like (green) regions are illustrated for *w*MelCS, *w*Mel, *w*SYT clade, and *w*Pip. Characteristics of each region are listed next to the genome schematic. Notably, the wMelCS genome, representative of the dynamic wMelPop, is distinguished from other variants by intact, flanking reverse transcriptases of group II intron origin (RT) on both sides. wPip, the only *Wolbachia* Supergroup B variant, is the most divergent and not associated with an RT, MutL or ankyrin repeat. Rather it is adjacent to WP1349, another gene that has been horizontally transferred between phage and arthropod [71].

S11 Fig. Prophage WO encodes a putative lytic cassette. Adjacent to the tail module of most prophage WO variants are three phage lysis candidates: ankyrin repeat containing protein (not shown), holin-like, and patatin-like phospholipase. (a) Similar to canonical holins, the prophage WO gene product encodes a single N-terminal transmembrane domain with no predicted charge. It is smaller than 150 amino acid residues, features a C-terminal coiled coil motif, and has a highly charged C-terminal domain. Unlike canonical holins, however, it is adjacent to a patatin-like gene rather than a characterized endolysin. (b) The prophage WO holin-like peptide shares 41.1% amino acid identity to a homolog in the non-*Wolbachia* prophage from the Tara Oceans Project that is directly adjacent to a GH108 lysozyme (complete genome illustrated in Fig 6). (c) A Mauve alignment of these genomic regions (core phage modules only; EAM not included) indicates 50.3% nucleotide identity across the majority of the sequence, including the holin-like gene (marked with a gold star). The similarity of these prophages suggest that prophage WO may utilize a similar holin-like gene with a different lytic enzyme (i.e., patatin rather than lysozyme) to lyse the bacterial cell.

S12 Fig. *Wolbachia* contains both prophage regions and GTA-like genes scattered through the chromosome. (a) Circular *w*Mel contains three prophage WO-like regions (teal) and multiple genes with homology to GTAs (orange) scattered throughout the genome, illustrated relative to the putative origin of replication (*ori*, gray). The Undecim Cluster is highlighted in navy blue, *cifA;B* are highlighted in pink, and *wmk* is highlighted in purple. (b) GTAs are present in at least one strain of each *Wolbachia* Supergroup except Supergroups J and L. They are also present in closely related Anaplasmataceae genera.

S13 Fig. Distance matrices of GTA nucleotide homology indicate evolution with the *Wolbachia* chromosome. Nucleotide alignments of GTA genes (a) portal, (b) BRO599, (c) TIM barrel, (d) major capsid, (e) head-tail connector, and (f) terminase indicate strict delineation based on *Wolbachia* supergroup. This supports evolution with the *Wolbachia* chromosome rather than independent evolution of a phage genome.

Supplementary Tables

S1 Table. Prophage WO genes are associated with arthropod-infecting *Wolbachia*. *Wolbachia* genomes are listed according to (A) host phylum; (B) *Wolbachia* supergroup; (C) *Wolbachia* name (D) host species and (E) host strain/lineage, if applicable; (F) NCBI accession number; (G) genome assembly status; (H) identification of prophage WO core genes; (I) identification of CI genes; and (J) identification of the Undecim Cluster. *Wolbachia* strains that did not include official names in the assembly reports are listed here using a capital letter for host genus and two to three lowercase letters for host species. "Highly pseudogenized" in column H indicates that the prophage genome is highly pseudogenized and encodes very few Core WO genes. (*) indicates that the genome lacks a complete Undecim Cluster but encodes WD0616 and/or WD0621 homologs. (**) indicates that the genome was not included as Source Data for Fig 1b due to incomplete genome information.

S2 Table. *w*Mhie encodes prophage WO genes. *w*Mhie, a *Wolbachia* endosymbiont from the nematode *Madathamugadia hiepei*, encodes four genes that are conserved throughout phage WO's transcriptional regulation and replication/repair modules. Each gene is listed by locus tag, annotation, and nucleotide homology to prophage WOVitA1.

967

968 **S3 Table. cifA and *cifB* genes are associated with *Wolbachia* Supergroups F and T.** *cifA* and
969 *cifB* are identified in Supergroups F and T. NCBI accession numbers and genomic coordinates (or
970 locus tags) are provided for each locus.

971

972 **S4 Table. Diversity of prophage WO mobile elements.** All mobile elements, both flanking and
973 internal, are listed for each prophage WO genome according to original genome annotations and
974 ISFinder [102]. The sr1WO group and WOVitA1-like prophages of the sr2WO group do not
975 feature transposases on the 5'- and 3'- flanking regions. The WORiA-like prophages of the sr2WO
976 group are associated with 3'- transposases; these correlate with putative truncations of the
977 prophage regions. Most genomes within the sr3WO group feature mobile elements on both 5'- and
978 3'- ends. IS refers to Insertion Sequence Family; RT refers to reverse transcriptase of group II
979 intron origin; Rpn refers to recombination promoting nuclease. (*) indicates a sequencing gap or
980 artificial join in the *Wolbachia* genome. Complete sequence information is unknown. (**)
981 indicates that these prophage sequences were obtained from contigs and may be segmented in the
982 *Wolbachia* chromosome; the exact 5' and 3' ends are uncertain. Genomic locations for each mobile
983 element are illustrated in S1-S7 Figs.

984

985 **S5 Table. *Wolbachia* GTA genes.** The annotation of *Wolbachia*'s distributed GTA genes is based
986 on a BLASTP against NCBI Conserved Domains; E-values are listed in column B.

987

988

Supplementary Text

S1 Text: Phage WO Structural Modules.

Phage WO structural genes are organized into head, connector/baseplate, tail, and tail fiber modules. The predicted function of each gene is discussed based on conserved protein domains and homology to other model systems, including lambda, T4, P2, and Mu phages.

Acknowledgements

We would like to thank Evelien Adriaenssens for helpful guidance with the taxonomic classification of prophage regions.

Author Contributions

Contributor Role	Role Definition
Conceptualization	Sarah Bordenstein and Seth Bordenstein
Data Curation	Sarah Bordenstein
Formal Analysis	Sarah Bordenstein and Seth Bordenstein
Funding Acquisition	Seth Bordenstein
Investigation	Sarah Bordenstein
Methodology	Sarah Bordenstein and Seth Bordenstein
Project Administration	Sarah Bordenstein
Resources	Sarah Bordenstein and Seth Bordenstein
Software	Sarah Bordenstein
Supervision	Sarah Bordenstein and Seth Bordenstein
Validation	Sarah Bordenstein and Seth Bordenstein
Visualization	Sarah Bordenstein
Writing – Original Draft Preparation	Sarah Bordenstein
Writing – Review & Editing	Sarah Bordenstein and Seth Bordenstein

List of Abbreviations

CI – cytoplasmic incompatibility

EAM – eukaryotic association module

GTA – gene transfer agent

ICTV - International Committee on Taxonomy of Viruses

IS – insertion sequence

HTH – helix-turn-helix

NCBI – National Center for Biotechnology Information

Rpn – recombination-promotion nuclease

RT – reverse transcriptase of group II intron origin

VNTR – variable number tandem repeat

WO-PC1 – WO protein cluster 1

WO-PC2 – WO protein cluster 2

References

1. Newton IL, Bordenstein SR. Correlations between bacterial ecology and mobile DNA. Curr Microbiol. 2011;62(1):198-208. doi: 10.1007/s00284-010-9693-3. pmid: 20577742

2. Cerveau N, Leclercq S, Leroy E, Bouchon D, Cordaux R. Short- and long-term evolutionary dynamics of bacterial insertion sequences: insights from *Wolbachia* endosymbionts. Genome Biol Evol. 2011;3:1175-86. doi: 10.1093/gbe/evr096. pmid: 21940637

3. Masui S, Kamoda S, Sasaki T, Ishikawa H. Distribution and evolution of bacteriophage WO in *Wolbachia*, the endosymbiont causing sexual alterations in arthropods. J Mol Evol. 2000;51(5):491-7. doi: 10.1007/s002390010112. pmid: 11080372

4. Kent BN, Bordenstein SR. Phage WO of *Wolbachia*: lambda of the endosymbiont world. Trends Microbiol. 2010;18(4):173-81. doi: 10.1016/j.tim.2009.12.011. pmid: 20083406

5. Reveillaud J, Bordenstein SR, Cruaud C, Shaiber A, Esen OC, Weill M, et al. The *Wolbachia* mobilome in *Culex pipiens* includes a putative plasmid. Nat Commun. 2019;10(1):1051. doi: 10.1038/s41467-019-08973-w. pmid: 30837458

6. Baiao GC, Janice J, Galinou M, Klasson L. Comparative genomics reveals factors associated with phenotypic expression of *Wolbachia*. Genome Biol Evol. 2021. doi: 10.1093/gbe/evab111. pmid: 34003269

7. Kaur R, Shropshire JD, Cross KL, Leigh B, Mansueto AJ, Stewart V, et al. Living in the endosymbiotic world of *Wolbachia*: A centennial review. Cell Host Microbe. 2021;29(6):879-93. doi: 10.1016/j.chom.2021.03.006. pmid: 33945798

8. Weinert LA, Araujo-Jnr EV, Ahmed MZ, Welch JJ. The incidence of bacterial endosymbionts in terrestrial arthropods. Proc Biol Sci. 2015;282(1807):20150249. doi: doi:10.1098/rspb.2015.0249. pmid: 25904667

9. Pruneau L, Moumene A, Meyer DF, Marcelino I, Lefrancois T, Vachiery N. Understanding *Anaplasmataceae* pathogenesis using "Omics" approaches. Front Cell Infect Microbiol. 2014;4:86. doi: 10.3389/fcimb.2014.00086. pmid: 25072029

10. Vavre F, Fleury F, Lepetit D, Fouillet P, Bouletreau M. Phylogenetic evidence for horizontal transmission of *Wolbachia* in host-parasitoid associations. Mol Biol Evol. 1999;16(12):1711-23. doi: 10.1093/oxfordjournals.molbev.a026084. pmid: 10605113

11. Boyle L, O'Neill SL, Robertson HM, Karr TL. Interspecific and intraspecific horizontal transfer of *Wolbachia* in *Drosophila*. Science. 1993;260(5115):1796-9. doi: 10.1126/science.8511587. pmid: 8511587

12. Chafee ME, Funk DJ, Harrison RG, Bordenstein SR. Lateral phage transfer in obligate intracellular bacteria (*Wolbachia*): verification from natural populations. Mol Biol Evol. 2010;27(3):501-5. doi: 10.1093/molbev/msp275. pmid: 19906794

13. Wang N, Jia S, Xu H, Liu Y, Huang D. Multiple Horizontal Transfers of Bacteriophage WO and Host *Wolbachia* in Fig Wasps in a Closed Community. Front Microbiol. 2016;7:136. doi: 10.3389/fmicb.2016.00136. pmid: 26913026

14. Kent BN, Salichos L, Gibbons JG, Rokas A, Newton IL, Clark ME, et al. Complete bacteriophage transfer in a bacterial endosymbiont (*Wolbachia*) determined by targeted genome capture. Genome Biol Evol. 2011;3:209-18. doi: 10.1093/gbe/evr007. pmid: 21292630

15. Gavotte L, Henri H, Stouthamer R, Charif D, Charlat S, Bouletreau M, et al. A Survey of the bacteriophage WO in the endosymbiotic bacteria *Wolbachia*. Mol Biol Evol. 2007;24(2):427-35. doi: 10.1093/molbev/msl171. pmid: 17095536

16. Bordenstein SR, Wernegreen JJ. Bacteriophage flux in endosymbionts (*Wolbachia*): infection frequency, lateral transfer, and recombination rates. Mol Biol Evol. 2004;21(10):1981-91. doi: 10.1093/molbev/msh211. pmid: 15254259

17. Ishmael N, Dunning Hotopp JC, Ioannidis P, Biber S, Sakamoto J, Siozios S, et al. Extensive genomic diversity of closely related *Wolbachia* strains. Microbiology. 2009;155(Pt 7):2211-22. doi: 10.1099/mic.0.027581-0. pmid: 19389774

18. Kent BN, Funkhouser LJ, Setia S, Bordenstein SR. Evolutionary genomics of a temperate bacteriophage in an obligate intracellular bacteria (*Wolbachia*). PLoS One. 2011;6(9):e24984. doi: 10.1371/journal.pone.0024984. pmid: 21949820

19. Klasson L, Westberg J, Sapountzis P, Naslund K, Lutnaes Y, Darby AC, et al. The mosaic genome structure of the *Wolbachia w*Ri strain infecting *Drosophila simulans*. Proc Natl Acad Sci U S A. 2009;106(14):5725-30. doi: 10.1073/pnas.0810753106. pmid: 19307581

20. Sanogo YO, Dobson SL. WO bacteriophage transcription in *Wolbachia*-infected *Culex pipiens*. Insect Biochem Mol Biol. 2006;36(1):80-5. doi: 10.1016/j.ibmb.2005.11.001. pmid: 16360953

21. Werren JH, Baldo L, Clark ME. *Wolbachia*: master manipulators of invertebrate biology. Nat Rev Microbiol. 2008;6(10):741-51. doi: 10.1038/nrmicro1969. pmid: 18794912

22. Charlat S, Hurst GD, Mercot H. Evolutionary consequences of *Wolbachia* infections. Trends Genet. 2003;19(4):217-23. doi: 10.1016/S0168-9525(03)00024-6. pmid: 12683975

23. Fenn K, Blaxter M. *Wolbachia* genomes: revealing the biology of parasitism and mutualism. Trends Parasitol. 2006;22(2):60-5. doi: 10.1016/j.pt.2005.12.012. pmid: 16406333

24. Slatko BE, Taylor MJ, Foster JM. The *Wolbachia* endosymbiont as an anti-filarial nematode target. Symbiosis. 2010;51(1):55-65. doi: 10.1007/s13199-010-0067-1. pmid: 20730111

25. Yamada R, Iturbe-Ormaetxe I, Brownlie JC, O'Neill SL. Functional test of the influence of *Wolbachia* genes on cytoplasmic incompatibility expression in *Drosophila melanogaster*. Insect Mol Biol. 2011;20(1):75-85. doi: 10.1111/j.1365-2583.2010.01042.x. pmid: 20854481

26. Sinkins SP, Walker T, Lynd AR, Steven AR, Makepeace BL, Godfray HC, et al. *Wolbachia* variability and host effects on crossing type in *Culex* mosquitoes. Nature. 2005;436(7048):257-60. doi: 10.1038/nature03629. pmid: 16015330

27. Duron O, Fort P, Weill M. Hypervariable prophage WO sequences describe an unexpected high number of *Wolbachia* variants in the mosquito *Culex pipiens*. Proc Biol Sci. 2006;273(1585):495-502. doi: 10.1098/rspb.2005.3336. pmid: 16615218

28. Duron O, Bernard C, Unal S, Berthomieu A, Berticat C, Weill M. Tracking factors modulating cytoplasmic incompatibilities in the mosquito *Culex pipiens*. Mol Ecol. 2006;15(10):3061-71. doi: 10.1111/j.1365-294X.2006.02996.x. pmid: 16911221

29. LePage DP, Metcalf JA, Bordenstein SR, On J, Perlmutter JI, Shropshire JD, et al. Prophage WO genes recapitulate and enhance *Wolbachia*-induced cytoplasmic incompatibility. Nature. 2017;543(7644):243-7. doi: 10.1038/nature21391. pmid: 28241146

30. Shropshire JD, On J, Layton EM, Zhou H, Bordenstein SR. One prophage WO gene rescues cytoplasmic incompatibility in *Drosophila melanogaster*. Proc Natl Acad Sci U S A. 2018;115(19):4987-91. doi: 10.1073/pnas.1800650115. pmid: 29686091

31. Chen H, Ronau JA, Beckmann JF, Hochstrasser M. A *Wolbachia* nuclease and its binding partner provide a distinct mechanism for cytoplasmic incompatibility. Proc Natl Acad Sci U S A. 2019;116(44):22314-21. doi: 10.1073/pnas.1914571116. pmid: 31615889

32. Beckmann JF, Ronau JA, Hochstrasser M. A *Wolbachia* deubiquitylating enzyme induces cytoplasmic incompatibility. Nat Microbiol. 2017;2:17007. doi: 10.1038/nmicrobiol.2017.7. pmid: 28248294

33. Perlmutter JI, Bordenstein SR, Unckless RL, LePage DP, Metcalf JA, Hill T, et al. The phage gene *wmk* is a candidate for male killing by a bacterial endosymbiont. PLoS Pathog. 2019;15(9):e1007936. doi: 10.1371/journal.ppat.1007936. pmid: 31504075

34. Bordenstein SR, Marshall ML, Fry AJ, Kim U, Wernegreen JJ. The tripartite associations between bacteriophage, *Wolbachia*, and arthropods. PLoS Pathog. 2006;2(5):e43. doi: 10.1371/journal.ppat.0020043. pmid: 16710453

35. Wright JD, Sjostrand FS, Portaro JK, Barr AR. The ultrastructure of the rickettsia-like microorganism *Wolbachia pipientis* and associated virus-like bodies in the mosquito *Culex pipiens*. J Ultrastruct Res. 1978;63(1):79-85. doi: 10.1016/s0022-5320(78)80046-x pmid: 671578

36. Biliske JA, Batista PD, Grant CL, Harris HL. The bacteriophage WORiC is the active phage element in *w*Ri of *Drosophila simulans* and represents a conserved class of WO phages. BMC Microbiol. 2011;11:251. doi: 10.1186/1471-2180-11-251. pmid: 22085419

37. Fujii Y, Kubo T, Ishikawa H, Sasaki T. Isolation and characterization of the bacteriophage WO from *Wolbachia*, an arthropod endosymbiont. Biochem Biophys Res Commun. 2004;317(4):1183-8. doi: 10.1016/j.bbrc.2004.03.164. pmid: 15094394

38. Tanaka K, Furukawa S, Nikoh N, Sasaki T, Fukatsu T. Complete WO phage sequences reveal their dynamic evolutionary trajectories and putative functional elements required for integration into the *Wolbachia* genome. Appl Environ Microbiol. 2009;75(17):5676-86. doi: 10.1128/AEM.01172-09. pmid: 19592535

39. Bordenstein SR, Bordenstein SR. Eukaryotic association module in phage WO genomes from *Wolbachia*. Nat Commun. 2016;7:13155. doi: 10.1038/ncomms13155. pmid: 27727237

40. Iturbe-Ormaetxe I, Burke GR, Riegler M, O'Neill SL. Distribution, expression, and motif variability of ankyrin domain genes in *Wolbachia pipientis*. J Bacteriol. 2005;187(15):5136-45. doi: 10.1128/JB.187.15.5136-5145.2005. pmid: 16030207

41. Siozios S, Ioannidis P, Klasson L, Andersson SG, Braig HR, Bourtzis K. The diversity and evolution of *Wolbachia* ankyrin repeat domain genes. PLoS One. 2013;8(2):e55390. doi: 10.1371/journal.pone.0055390. pmid: 23390535

42. Jahn MT, Arkhipova K, Markert SM, Stigloher C, Lachnit T, Pita L, et al. A Phage Protein Aids Bacterial Symbionts in Eukaryote Immune Evasion. Cell Host Microbe. 2019;26(4):542-50 e5. doi: 10.1016/j.chom.2019.08.019. pmid: 31561965

43. National Library of Medicine (US) National Center for Biotechnology Information. National Center for Biotechnology Information (NCBI) Bethesda (MD)1988. Available from: https://www.ncbi.nlm.nih.gov/.

44. International Committee on Taxonomy of Viruses Executive Committee. The new scope of virus taxonomy: partitioning the virosphere into 15 hierarchical ranks. Nat Microbiol. 2020;5(5):668-74. doi: 10.1038/s41564-020-0709-x. pmid: 32341570

45. Simmonds P, Adams MJ, Benko M, Breitbart M, Brister JR, Carstens EB, et al. Consensus statement: Virus taxonomy in the age of metagenomics. Nat Rev Microbiol. 2017;15(3):161-8. doi: 10.1038/nrmicro.2016.177. pmid: 28134265

46. Lindsey ARI, Rice DW, Bordenstein SR, Brooks AW, Bordenstein SR, Newton ILG. Evolutionary Genetics of Cytoplasmic Incompatibility Genes *cifA* and *cifB* in Prophage WO of *Wolbachia*. Genome Biol Evol. 2018;10(2):434-51. doi: 10.1093/gbe/evy012. pmid: 29351633

47. Martinez J, Klasson L, Welch JJ, Jiggins FM. Life and Death of Selfish Genes: Comparative Genomics Reveals the Dynamic Evolution of Cytoplasmic Incompatibility. Mol Biol Evol. 2021;38(1):2-15. doi: 10.1093/molbev/msaa209. pmid: 32797213

48. Wu M, Sun LV, Vamathevan J, Riegler M, Deboy R, Brownlie JC, et al. Phylogenomics of the reproductive parasite *Wolbachia pipientis* *w*Mel: a streamlined genome overrun by mobile genetic elements. PLoS Biol. 2004;2(3):E69. doi: 10.1371/journal.pbio.0020069. pmid: 15024419

49. Crainey JL, Hurst J, Lamberton PHL, Cheke RA, Griffin CE, Wilson MD, et al. The Genomic Architecture of Novel *Simulium damnosum Wolbachia* Prophage Sequence Elements and Implications for Onchocerciasis Epidemiology. Front Microbiol. 2017;8:852. doi: 10.3389/fmicb.2017.00852. pmid: 28611731

50. Smith MCM. Phage-encoded Serine Integrases and Other Large Serine Recombinases. Microbiol Spectr. 2015;3(4). doi: 10.1128/microbiolspec.MDNA3-0059-2014. pmid: 26350324

51. Metcalf JA, Jo M, Bordenstein SR, Jaenike J, Bordenstein SR. Recent genome reduction of *Wolbachia* in *Drosophila recens* targets phage WO and narrows candidates for reproductive parasitism. PeerJ. 2014;2:e529. doi: 10.7717/peerj.529. pmid: 25165636

52. Newton IL, Clark ME, Kent BN, Bordenstein SR, Qu J, Richards S, et al. Comparative Genomics of Two Closely Related *Wolbachia* with Different Reproductive Effects on Hosts. Genome Biol Evol. 2016;8(5):1526-42. doi: 10.1093/gbe/evw096. pmid: 27189996

53. Riegler M, Iturbe-Ormaetxe I, Woolfit M, Miller WJ, O'Neill SL. Tandem repeat markers as novel diagnostic tools for high resolution fingerprinting of *Wolbachia*. BMC Microbiol. 2012;12 Suppl 1:S12. doi: 10.1186/1471-2180-12-S1-S12. pmid: 22375862

54. Duplouy A, Iturbe-Ormaetxe I, Beatson SA, Szubert JM, Brownlie JC, McMeniman CJ, et al. Draft genome sequence of the male-killing *Wolbachia* strain *w*Bol1 reveals recent horizontal gene transfers from diverse sources. BMC Genomics. 2013;14:20. doi: 10.1186/1471-2164-14-20. pmid: 23324387

55. Harshey RM. Transposable Phage Mu. Microbiol Spectr. 2014;2(5). doi: 10.1128/microbiolspec.MDNA3-0007-2014. pmid: 26104374

56. Kampfraath AA, Klasson L, Anvar SY, Vossen R, Roelofs D, Kraaijeveld K, et al. Genome expansion of an obligate parthenogenesis-associated *Wolbachia* poses an exception to the symbiont reduction model. BMC Genomics. 2019;20(1):106. doi: 10.1186/s12864-019-5492-9. pmid: 30727958

57. Bobay LM, Touchon M, Rocha EP. Pervasive domestication of defective prophages by bacteria. Proc Natl Acad Sci U S A. 2014;111(33):12127-32. doi: 10.1073/pnas.1405336111. pmid: 25092302

1184 58. Ramisetty BCM, Sudhakari PA. Bacterial 'Grounded' Prophages: Hotspots for Genetic
1185 Renovation and Innovation. Front Genet. 2019;10:65. doi: 10.3389/fgene.2019.00065. pmid:
1186 30809245
1187 59. Fillol-Salom A, Martinez-Rubio R, Abdulrahman RF, Chen J, Davies R, Penades JR. Phage-
1188 inducible chromosomal islands are ubiquitous within the bacterial universe. ISME J.
1189 2018;12(9):2114-28. doi: 10.1038/s41396-018-0156-3. pmid: 29875435
1190 60. Penades JR, Christie GE. The Phage-Inducible Chromosomal Islands: A Family of Highly
1191 Evolved Molecular Parasites. Annu Rev Virol. 2015;2(1):181-201. doi: 10.1146/annurev-
1192 virology-031413-085446. pmid: 26958912
1193 61. Ioannidis P, Dunning Hotopp JC, Sapountzis P, Siozios S, Tsiamis G, Bordenstein SR, et al.
1194 New criteria for selecting the origin of DNA replication in *Wolbachia* and closely related
1195 bacteria. BMC Genomics. 2007;8:182. doi: 10.1186/1471-2164-8-182. pmid: 17584494
1196 62. Rands CM, Brussow H, Zdobnov EM. Comparative genomics groups phages of
1197 *Negativicutes* and classical *Firmicutes* despite different Gram-staining properties. Environ
1198 Microbiol. 2019;21(11):3989-4001. doi: 10.1111/1462-2920.14746. pmid: 31314945
1199 63. Oliveira PH, Touchon M, Cury J, Rocha EPC. The chromosomal organization of horizontal
1200 gene transfer in bacteria. Nat Commun. 2017;8(1):841. doi: 10.1038/s41467-017-00808-w.
1201 pmid: 29018197
1202 64. Canchaya C, Fournous G, Brussow H. The impact of prophages on bacterial
1203 chromosomes. Mol Microbiol. 2004;53(1):9-18. doi: 10.1111/j.1365-2958.2004.04113.x. pmid:
1204 15225299
1205 65. Bobay LM, Rocha EP, Touchon M. The adaptation of temperate bacteriophages to their
1206 host genomes. Mol Biol Evol. 2013;30(4):737-51. doi: 10.1093/molbev/mss279. pmid:
1207 23243039
1208 66. Woolfit M, Iturbe-Ormaetxe I, Brownlie JC, Walker T, Riegler M, Seleznev A, et al.
1209 Genomic evolution of the pathogenic *Wolbachia* strain, *w*MelPop. Genome Biol Evol.
1210 2013;5(11):2189-204. doi: 10.1093/gbe/evt169. pmid: 24190075
1211 67. Duarte EH, Carvalho A, Lopez-Madrigal S, Costa J, Teixeira L. Forward genetics in
1212 *Wolbachia*: Regulation of *Wolbachia* proliferation by the amplification and deletion of an
1213 addictive genomic island. PLoS Genet. 2021;17(6):e1009612. doi:
1214 10.1371/journal.pgen.1009612. pmid: 34143770
1215 68. Rohrscheib CE, Frentiu FD, Horn E, Ritchie FK, van Swinderen B, Weible MW, 2nd, et al.
1216 Intensity of Mutualism Breakdown Is Determined by Temperature Not Amplification of
1217 *Wolbachia* Genes. PLoS Pathog. 2016;12(9):e1005888. doi: 10.1371/journal.ppat.1005888.
1218 pmid: 27661080
1219 69. Chrostek E, Teixeira L. Mutualism breakdown by amplification of *Wolbachia* genes. PLoS
1220 Biol. 2015;13(2):e1002065. doi: 10.1371/journal.pbio.1002065. pmid: 25668031
1221 70. Fallon AM. DNA recombination and repair in *Wolbachia*: RecA and related proteins. Mol
1222 Genet Genomics. 2021;296(2):437-56. doi: 10.1007/s00438-020-01760-z. pmid: 33507381
1223 71. Klasson L, Kambris Z, Cook PE, Walker T, Sinkins SP. Horizontal gene transfer between
1224 *Wolbachia* and the mosquito *Aedes aegypti*. BMC Genomics. 2009;10:33. doi: 10.1186/1471-
1225 2164-10-33. pmid: 19154594
1226 72. Chrostek E, Marialva MS, Esteves SS, Weinert LA, Martinez J, Jiggins FM, et al. *Wolbachia*
1227 variants induce differential protection to viruses in *Drosophila melanogaster*: a phenotypic and

phylogenomic analysis. PLoS Genet. 2013;9(12):e1003896. doi: 10.1371/journal.pgen.1003896. pmid: 24348259

73. Matsuura M, Saldanha R, Ma H, Wank H, Yang J, Mohr G, et al. A bacterial group II intron encoding reverse transcriptase, maturase, and DNA endonuclease activities: biochemical demonstration of maturase activity and insertion of new genetic information within the intron. Genes Dev. 1997;11(21):2910-24. doi: 10.1101/gad.11.21.2910. pmid: 9353259

74. Dong X, Qu G, Piazza CL, Belfort M. Group II intron as cold sensor for self-preservation and bacterial conjugation. Nucleic Acids Res. 2020;48(11):6198-209. doi: 10.1093/nar/gkaa313. pmid: 32379323

75. Baldridge GD, Markowski TW, Witthuhn BA, Higgins L, Baldridge AS, Fallon AM. The *Wolbachia* WO bacteriophage proteome in the *Aedes albopictus* C/wStr1 cell line: evidence for lytic activity? In Vitro Cell Dev Biol Anim. 2016;52(1):77-88. doi: 10.1007/s11626-015-9949-0. pmid: 26427709

76. Gillespie JJ, Joardar V, Williams KP, Driscoll T, Hostetler JB, Nordberg E, et al. A *Rickettsia* genome overrun by mobile genetic elements provides insight into the acquisition of genes characteristic of an obligate intracellular lifestyle. J Bacteriol. 2012;194(2):376-94. doi: 10.1128/JB.06244-11. pmid: 22056929

77. Gutzwiller F, Carmo CR, Miller DE, Rice DW, Newton IL, Hawley RS, et al. Dynamics of *Wolbachia pipientis* Gene Expression Across the *Drosophila melanogaster* Life Cycle. G3 (Bethesda). 2015;5(12):2843-56. doi: 10.1534/g3.115.021931. pmid: 26497146

78. Masui S, Kuroiwa H, Sasaki T, Inui M, Kuroiwa T, Ishikawa H. Bacteriophage WO and virus-like particles in *Wolbachia*, an endosymbiont of arthropods. Biochem Biophys Res Commun. 2001;283(5):1099-104. doi: 10.1006/bbrc.2001.4906. pmid: 11355885

79. Young R. Bacteriophage lysis: mechanism and regulation. Microbiol Rev. 1992;56(3):430-81. pmid: 1406491

80. Otten C, Brilli M, Vollmer W, Viollier PH, Salje J. Peptidoglycan in obligate intracellular bacteria. Mol Microbiol. 2018;107(2):142-63. doi: 10.1111/mmi.13880. pmid: 29178391

81. Bordenstein SR, Bordenstein SR. Temperature affects the tripartite interactions between bacteriophage WO, *Wolbachia*, and cytoplasmic incompatibility. PLoS One. 2011;6(12):e29106. doi: 10.1371/journal.pone.0029106. pmid: 22194999

82. Rahman MS, Ammerman NC, Sears KT, Ceraul SM, Azad AF. Functional characterization of a phospholipase A(2) homolog from *Rickettsia typhi*. J Bacteriol. 2010;192(13):3294-303. doi: 10.1128/JB.00155-10. pmid: 20435729

83. Sato H, Frank DW. ExoU is a potent intracellular phospholipase. Mol Microbiol. 2004;53(5):1279-90. doi: 10.1111/j.1365-2958.2004.04194.x. pmid: 15387809

84. Banerji S, Flieger A. Patatin-like proteins: a new family of lipolytic enzymes present in bacteria? Microbiology. 2004;150(Pt 3):522-5. doi: 10.1099/mic.0.26957-0. pmid: 14993300

85. Kamilla S, Jain V. Mycobacteriophage D29 holin C-terminal region functionally assists in holin aggregation and bacterial cell death. FEBS J. 2016;283(1):173-90. doi: 10.1111/febs.13565. pmid: 26471254

86. Wang IN, Smith DL, Young R. Holins: the protein clocks of bacteriophage infections. Annu Rev Microbiol. 2000;54:799-825. doi: 10.1146/annurev.micro.54.1.799. pmid: 11018145

87. Lang AS, Beatty JT. Genetic analysis of a bacterial genetic exchange element: the gene transfer agent of *Rhodobacter capsulatus*. Proc Natl Acad Sci U S A. 2000;97(2):859-64. doi: 10.1073/pnas.97.2.859 pmid: 10639170

88. Westbye AB, Beatty JT, Lang AS. Guaranteeing a captive audience: coordinated regulation of gene transfer agent (GTA) production and recipient capability by cellular regulators. Curr Opin Microbiol. 2017;38:122-9. doi: 10.1016/j.mib.2017.05.003. pmid: 28599143

89. Lang AS, Beatty JT. Importance of widespread gene transfer agent genes in alpha-proteobacteria. Trends Microbiol. 2007;15(2):54-62. doi: 10.1016/j.tim.2006.12.001. pmid: 17184993

90. Dohra H, Tanaka K, Suzuki T, Fujishima M, Suzuki H. Draft genome sequences of three *Holospora* species (*Holospora obtusa*, *Holospora undulata*, and *Holospora elegans*), endonuclear symbiotic bacteria of the ciliate *Paramecium caudatum*. FEMS Microbiol Lett. 2014;359(1):16-8. doi: 10.1111/1574-6968.12577. pmid: 25115770

91. Kantor RS, Miller SE, Nelson KL. The Water Microbiome Through a Pilot Scale Advanced Treatment Facility for Direct Potable Reuse. Front Microbiol. 2019;10:993. doi: 10.3389/fmicb.2019.00993. pmid: 31139160

92. Tully BJ, Graham ED, Heidelberg JF. The reconstruction of 2,631 draft metagenome-assembled genomes from the global oceans. Sci Data. 2018;5:170203. doi: 10.1038/sdata.2017.203. pmid: 29337314

93. Egan S, Gardiner M. Microbial Dysbiosis: Rethinking Disease in Marine Ecosystems. Front Microbiol. 2016;7:991. doi: 10.3389/fmicb.2016.00991. pmid: 27446031

94. Takano SI, Gotoh Y, Hayashi T. "*Candidatus* Mesenet longicola": Novel Endosymbionts of *Brontispa longissima* that Induce Cytoplasmic Incompatibility. Microb Ecol. 2021. doi: 10.1007/s00248-021-01686-y. pmid: 33454808

95. Rocchi I, Ericson CF, Malter KE, Zargar S, Eisenstein F, Pilhofer M, et al. A Bacterial Phage Tail-like Structure Kills Eukaryotic Cells by Injecting a Nuclease Effector. Cell Rep. 2019;28(2):295-301 e4. doi: 10.1016/j.celrep.2019.06.019. pmid: 31291567

96. Gillespie JJ, Driscoll TP, Verhoeve VI, Rahman MS, Macaluso KR, Azad AF. A Tangled Web: Origins of Reproductive Parasitism. Genome Biol Evol. 2018;10(9):2292-309. doi: 10.1093/gbe/evy159. pmid: 30060072

97. Garushyants SK, Beliavskaia AY, Malko DB, Logacheva MD, Rautian MS, Gelfand MS. Comparative Genomic Analysis of *Holospora* spp., Intranuclear Symbionts of Paramecia. Front Microbiol. 2018;9:738. doi: 10.3389/fmicb.2018.00738. pmid: 29713316

98. Zdobnov EM, Apweiler R. InterProScan--an integration platform for the signature-recognition methods in InterPro. Bioinformatics. 2001;17(9):847-8. doi: 10.1093/bioinformatics/17.9.847. pmid: 11590104

99. Altschul SF, Gish W, Miller W, Myers EW, Lipman DJ. Basic local alignment search tool. J Mol Biol. 1990;215(3):403-10. doi: 10.1016/S0022-2836(05)80360-2. pmid: 2231712

100. Finn RD, Bateman A, Clements J, Coggill P, Eberhardt RY, Eddy SR, et al. Pfam: the protein families database. Nucleic Acids Res. 2014;42(Database issue):D222-30. doi: 10.1093/nar/gkt1223. pmid: 24288371

101. Soding J, Biegert A, Lupas AN. The HHpred interactive server for protein homology detection and structure prediction. Nucleic Acids Res. 2005;33(Web Server issue):W244-8. doi: 10.1093/nar/gki408. pmid: 15980461

102. Siguier P, Perochon J, Lestrade L, Mahillon J, Chandler M. ISfinder: the reference centre for bacterial insertion sequences. Nucleic Acids Res. 2006;34(Database issue):D32-6. doi: 10.1093/nar/gkj014. pmid: 16381877

103. Schultz J, Copley RR, Doerks T, Ponting CP, Bork P. SMART: a web-based tool for the study of genetically mobile domains. Nucleic Acids Res. 2000;28(1):231-4. doi: 10.1093/nar/28.1.231. pmid: 10592234

104. Darling AC, Mau B, Blattner FR, Perna NT. Mauve: multiple alignment of conserved genomic sequence with rearrangements. Genome Res. 2004;14(7):1394-403. doi: 10.1101/gr.2289704. pmid: 15231754

105. Edgar RC. MUSCLE: multiple sequence alignment with high accuracy and high throughput. Nucleic Acids Res. 2004;32(5):1792-7. doi: 10.1093/nar/gkh340. pmid: 15034147

106. Darriba D, Taboada GL, Doallo R, Posada D. ProtTest 3: fast selection of best-fit models of protein evolution. Bioinformatics. 2011;27(8):1164-5. doi: 10.1093/bioinformatics/btr088. pmid: 21335321

107. Guindon S, Gascuel O. A simple, fast, and accurate algorithm to estimate large phylogenies by maximum likelihood. Syst Biol. 2003;52(5):696-704. doi: 10.1080/10635150390235520. pmid: 14530136

108. Ronquist F, Teslenko M, van der Mark P, Ayres DL, Darling A, Hohna S, et al. MrBayes 3.2: efficient Bayesian phylogenetic inference and model choice across a large model space. Syst Biol. 2012;61(3):539-42. doi: 10.1093/sysbio/sys029. pmid: 22357727

109. Turner D, Kropinski AM, Adriaenssens EM. A Roadmap for Genome-Based Phage Taxonomy. Viruses. 2021;13(3):506. doi: 10.3390/v13030506 pmid: doi:10.3390/v13030506

110. Klasson L, Walker T, Sebaihia M, Sanders MJ, Quail MA, Lord A, et al. Genome evolution of *Wolbachia* strain *w*Pip from the *Culex pipiens* group. Mol Biol Evol. 2008;25(9):1877-87. doi: 10.1093/molbev/msn133. pmid: 18550617

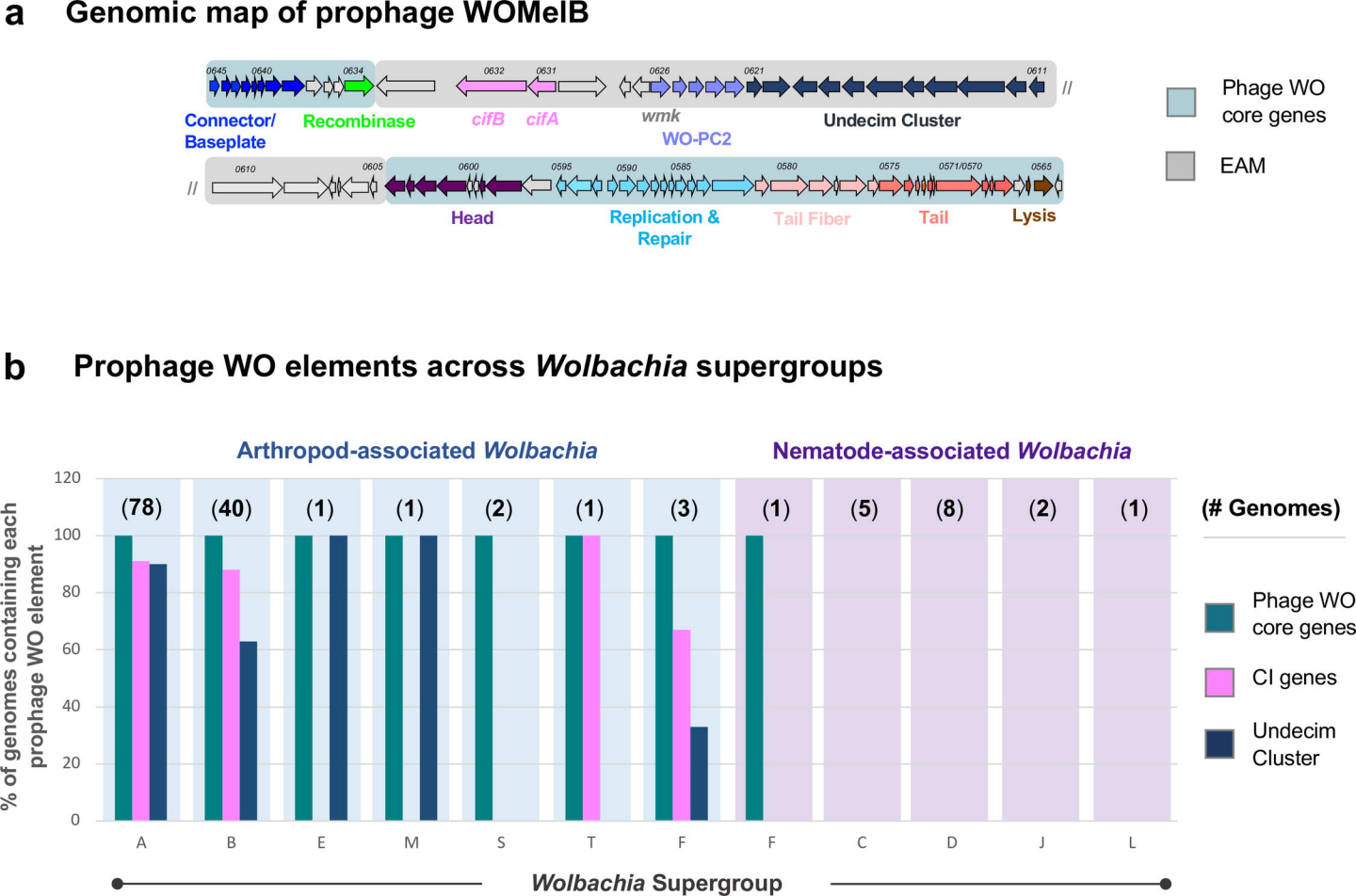
a
Genomic map of prophage WOMelB
0645
0640
0634
0632
0631
0626
0621
0611
Connector/
Baseplate
Recombinase
cifB
cifA
wmk
WO-PC2
Undecim Cluster
0610
0605
0600
0595
0590
0585
0580
0575
0571/0570
0565
Head
Replication &
Repair
Tail Fiber
Tail
Lysis
Phage WO
core genes
EAM
b
Prophage WO elements across Wolbachia supergroups
Arthropod-associated Wolbachia
Nematode-associated Wolbachia
% of genomes containing each
prophage WO element
120
100
80
60
40
20
0
(78)
(40)
(1)
(1)
(2)
(1)
(3)
(1)
(5)
(8)
(2)
(1)
(# Genomes)
A
B
E
M
S
T
F
F
C
D
J
L
Wolbachia Supergroup
Phage WO
core genes
CI genes
Undecim
Cluster

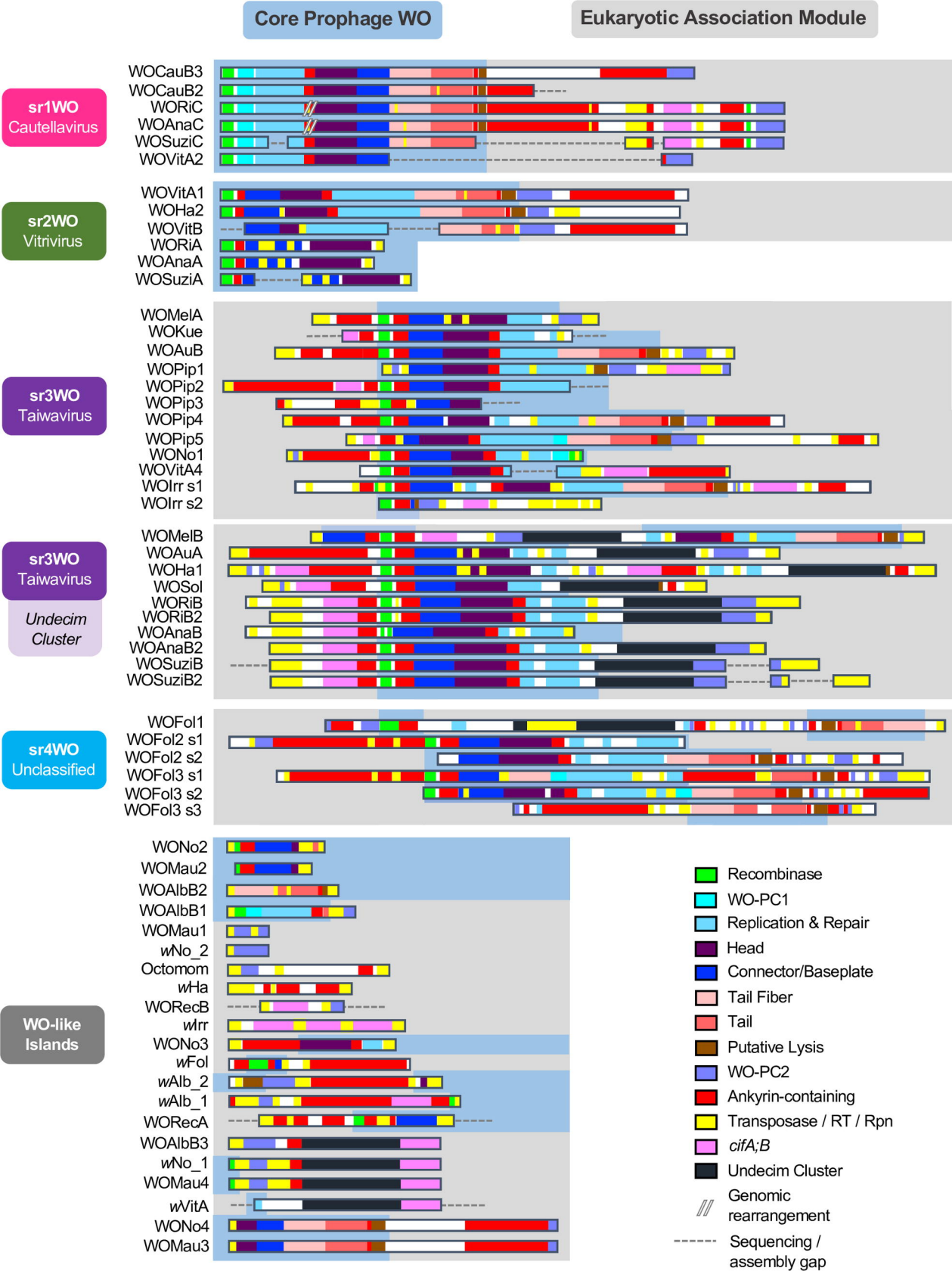
Core Prophage WO
Eukaryotic Association Module
sr1WO Cautellavirus
WOCauB3
WOCauB2
WORiC
WOAnaC
WOSuziC
WOVitA2
sr2WO Vitrivirus
WOVitA1
WOHa2
WOVitB
WORiA
WOAnaA
WOSuziA
sr3WO Taiwavirus
WOMelA
WOKue
WOAuB
WOPip1
WOPip2
WOPip3
WOPip4
WOPip5
WONo1
WOVitA4
WOIrr s1
WOIrr s2
sr3WO Taiwavirus
Undecim Cluster
WOMelB
WOAuA
WOHa1
WOSol
WORiB
WORiB2
WOAnaB
WOAnaB2
WOSuziB
WOSuziB2
sr4WO Unclassified
WOFol1
WOFol2 s1
WOFol2 s2
WOFol3 s1
WOFol3 s2
WOFol3 s3
WO-like Islands
WONo2
WOMau2
WOAlbB2
WOAlbB1
WOMau1
wNo_2
Octomom
wHa
WORecB
wIrr
WONo3
wFol
wAlb_2
wAlb_1
WORecA
WOAlbB3
wNo_1
WOMau4
wVitA
WONo4
WOMau3
Recombinase
WO-PC1
Replication & Repair
Head
Connector/Baseplate
Tail Fiber
Tail
Putative Lysis
WO-PC2
Ankyrin-containing
Transposase / RT / Rpn
cifA;B
Undecim Cluster
Genomic rearrangement
Sequencing / assembly gap

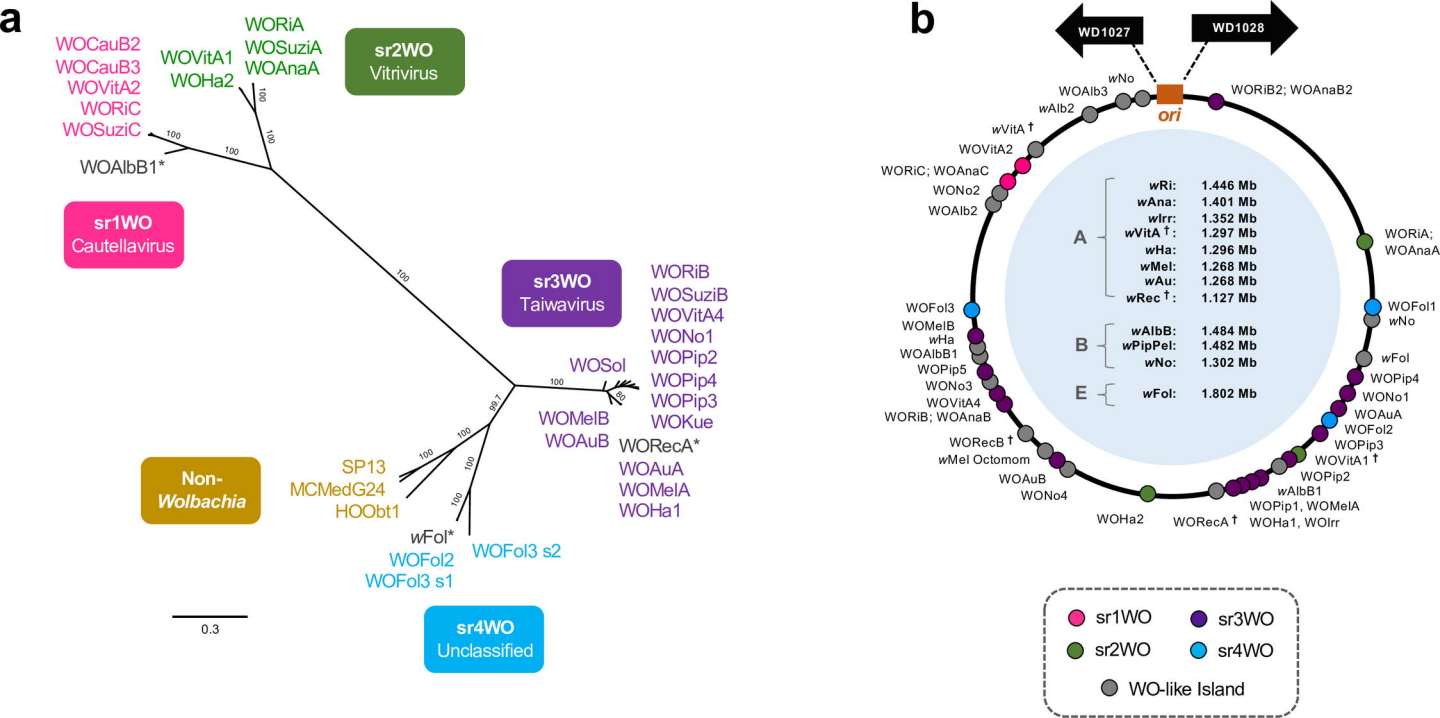
a
WOCauB2
WOCauB3
WOVitA2
WORiC
WOSuziC
WOAlbB1*
WORiA
WOSuziA
WOAnaA
WOVitA1
WOHa2
sr2WO
Vitrivirus
sr1WO
Cautellavirus
sr3WO
Taiwavirus
WORiB
WOSuziB
WOVitA4
WONo1
WOPip2
WOPip4
WOPip3
WOKue
WOSol
WOMelB
WOAuB
WORecA*
WOAuA
WOMelA
WOHa1
Non-
Wolbachia
SP13
MCMedG24
HOObt1
wFol*
WOFol2
WOFol3 s1
WOFol3 s2
sr4WO
Unclassified
0.3
100
99.7
85
b
WD1027
WD1028
ori
wNo
WOAlb3
WORiB2; WOAnaB2
wAlb2
wVitA †
WOVitA2
WORiC; WOAnaC
WONo2
WOAlb2
wRi: 1.446 Mb
wAna: 1.401 Mb
wIrr: 1.352 Mb
wVitA †: 1.297 Mb
wHa: 1.296 Mb
wMel: 1.268 Mb
wAu: 1.268 Mb
wRec †: 1.127 Mb
A
B
E
wAlbB: 1.484 Mb
wPipPel: 1.482 Mb
wNo: 1.302 Mb
wFol: 1.802 Mb
WORiA;
WOAnaA
WOFol1
wNo
WOFol3
WOMelB
wHa
WOAlbB1
WOPip5
WONo3
WOVitA4
WORiB; WOAnaB
wFol
WOPip4
WONo1
WOAuA
WOFol2
WOPip3
WOVitA1 †
WOPip2
wAlbB1
WOPip1, WOMelA
WOHa1, WOIrr
WORecA †
WOHa2
WOAuB
WONo4
WORecB †
wMel Octomom
sr1WO
sr2WO
sr3WO
sr4WO
WO-like Island

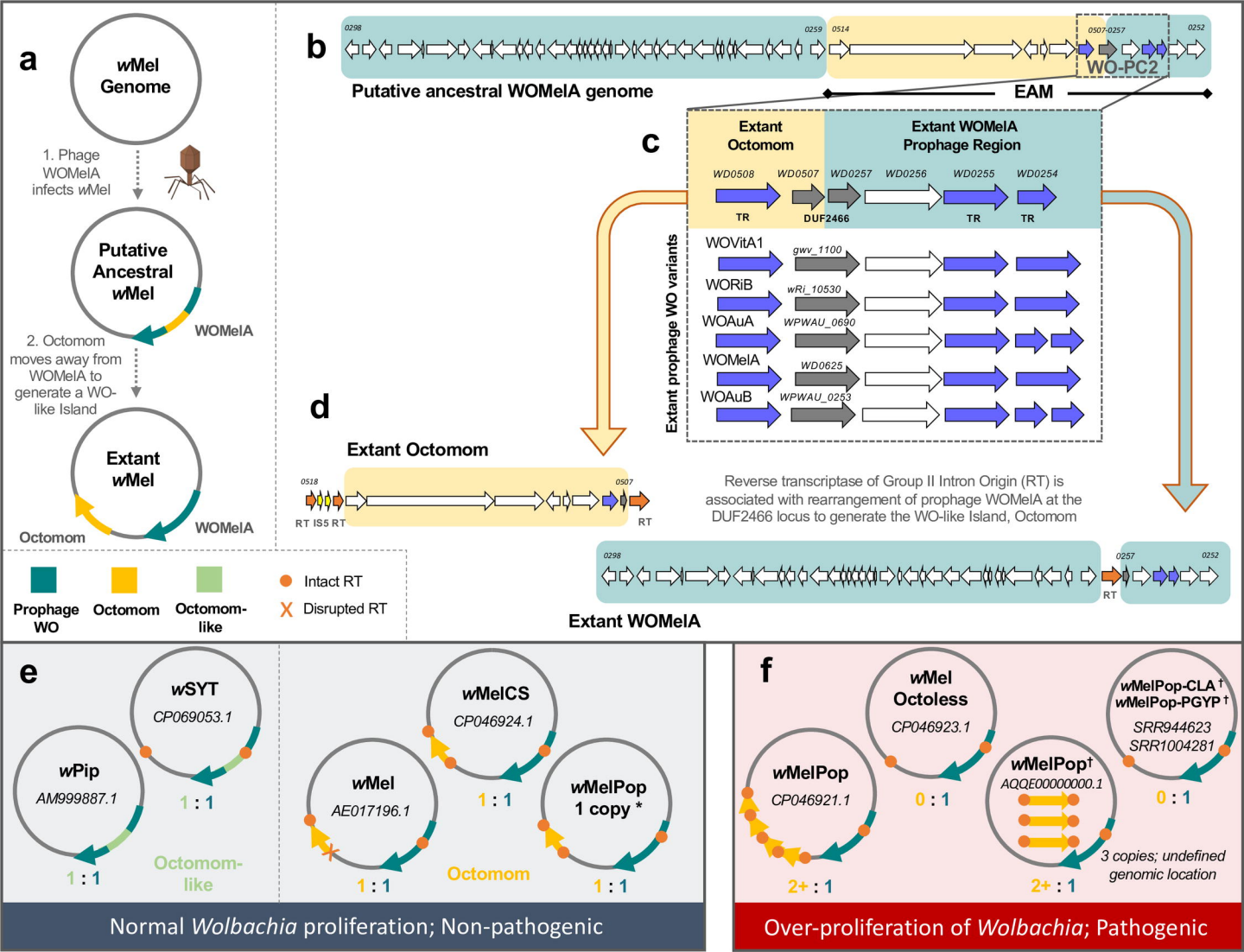
a
wMel Genome
1. Phage WOMelA infects wMel
Putative Ancestral wMel
WOMelA
2. Octomom moves away from WOMelA to generate a WO-like Island
Extant wMel
WOMelA
Octomom
b
Putative ancestral WOMelA genome
0298
0259
0514
0507-0257
0252
WO-PC2
EAM
c
Extant Octomom
Extant WOMelA Prophage Region
WD0508
WD0507
WD0257
WD0256
WD0255
WD0254
TR
DUF2466
TR
TR
Extant prophage WO variants
WOVitA1
gwv_1100
WORiB
wRi_10530
WOAuA
WPWAU_0690
WOMelA
WD0625
WOAuB
WPWAU_0253
d
Extant Octomom
0518
0507
RT IS5 RT
RT
Reverse transcriptase of Group II Intron Origin (RT) is associated with rearrangement of prophage WOMelA at the DUF2466 locus to generate the WO-like Island, Octomom
0298
0257
0252
RT
Extant WOMelA
Prophage WO
Octomom
Octomom-like
Intact RT
Disrupted RT
e
wSYT
CP069053.1
wPip
AM999887.1
1 : 1
1 : 1
Octomom-like
wMelCS
CP046924.1
wMel
AE017196.1
wMelPop
1 copy *
1 : 1
1 : 1
Octomom
1 : 1
Normal Wolbachia proliferation; Non-pathogenic
f
wMel Octoless
CP046923.1
wMelPop
CP046921.1
0 : 1
2+ : 1
wMelPop†
AQQE00000000.1
2+ : 1
wMelPop-CLA †
wMelPop-PGYP †
SRR944623
SRR1004281
0 : 1
3 copies; undefined genomic location
Over-proliferation of Wolbachia; Pathogenic

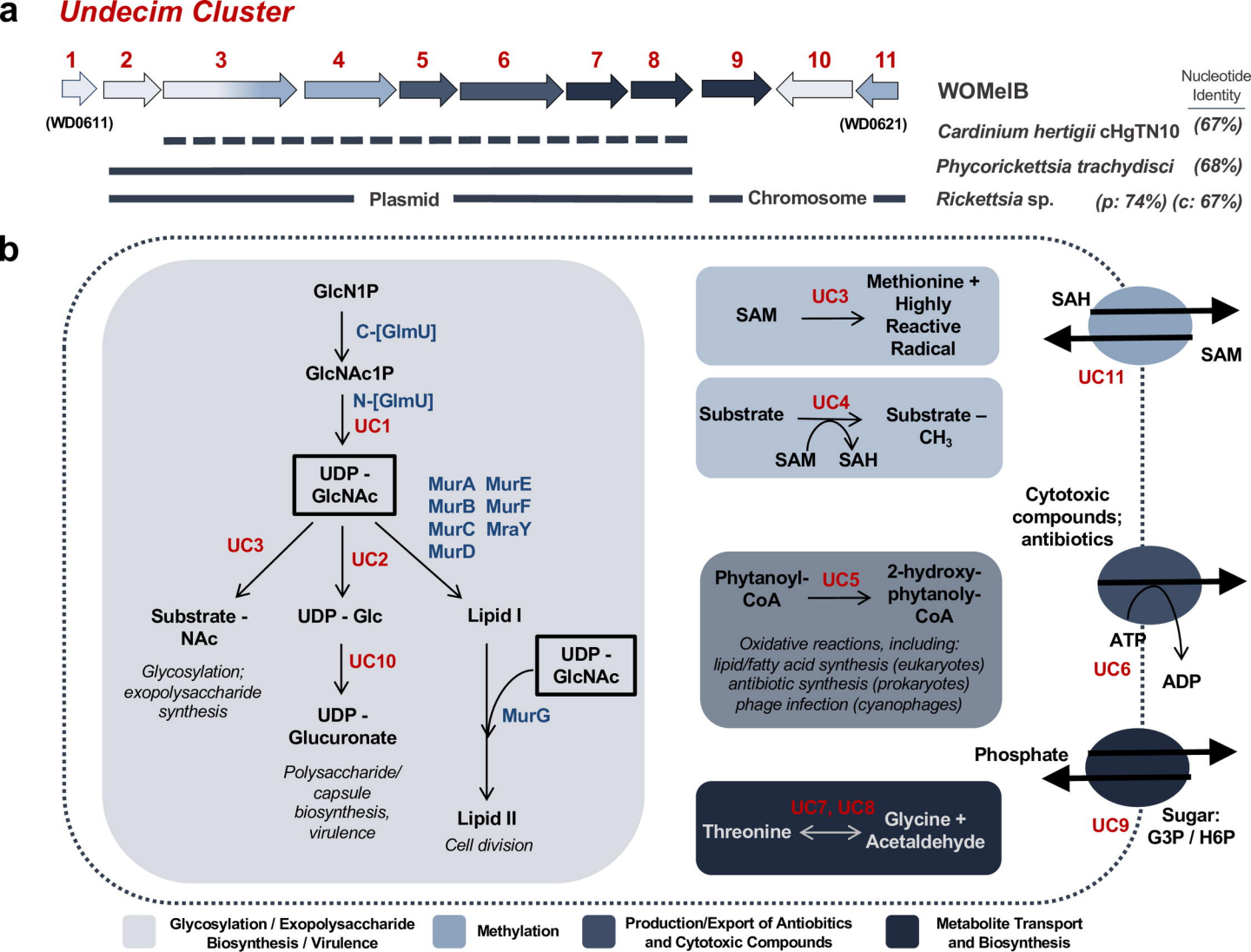
a
Undecim Cluster
1
2
3
4
5
6
7
8
9
10
11
(WD0611)
(WD0621)
Plasmid
Chromosome
WOMelB
Nucleotide Identity
Cardinium hertigii cHgTN10 (67%)
Phycorickettsia trachydisci (68%)
Rickettsia sp. (p: 74%) (c: 67%)
b
GlcN1P
C-[GlmU]
GlcNAc1P
N-[GlmU]
UC1
UDP - GlcNAc
MurA MurE
MurB MurF
MurC MraY
MurD
UC3
UC2
Substrate - NAc
Glycosylation; exopolysaccharide synthesis
UDP - Glc
UC10
UDP - Glucuronate
Polysaccharide/ capsule biosynthesis, virulence
Lipid I
UDP - GlcNAc
MurG
Lipid II
Cell division
SAM
UC3
Methionine + Highly Reactive Radical
Substrate
UC4
Substrate – CH3
SAM
SAH
Phytanoyl-CoA
UC5
2-hydroxy-phytanoly-CoA
Oxidative reactions, including: lipid/fatty acid synthesis (eukaryotes) antibiotic synthesis (prokaryotes) phage infection (cyanophages)
Threonine
UC7, UC8
Glycine + Acetaldehyde
SAH
SAM
UC11
Cytotoxic compounds; antibiotics
ATP
UC6
ADP
Phosphate
UC9
Sugar: G3P / H6P
Glycosylation / Exopolysaccharide Biosynthesis / Virulence
Methylation
Production/Export of Antiobitics and Cytotoxic Compounds
Metabolite Transport and Biosynthesis

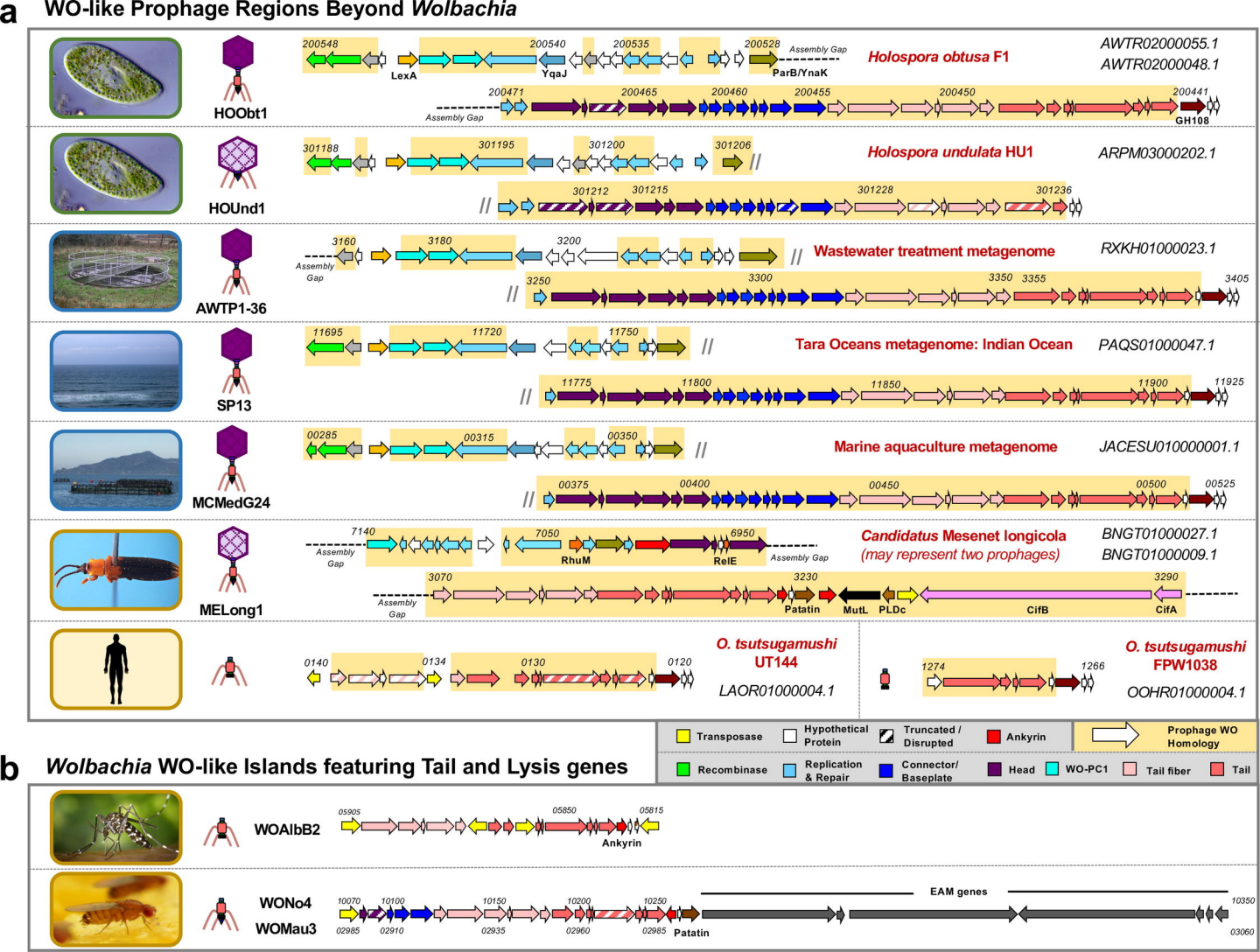
a
WO-like Prophage Regions Beyond Wolbachia
HOObt1
Holospora obtusa F1
AWTR02000055.1
AWTR02000048.1
200548
LexA
200540
YqaJ
200535
200528
Assembly Gap
ParB/YnaK
200471
Assembly Gap
200465
200460
200455
200450
200441
GH108
HOUnd1
Holospora undulata HU1
ARPM03000202.1
301188
301195
301200
301206
301212
301215
301228
301236
AWTP1-36
Wastewater treatment metagenome
RXKH01000023.1
3160
Assembly Gap
3180
3200
3250
3300
3350
3355
3405
SP13
Tara Oceans metagenome: Indian Ocean
PAQS01000047.1
11695
11720
11750
11775
11800
11850
11900
11925
MCMedG24
Marine aquaculture metagenome
JACESU010000001.1
00285
00315
00350
00375
00400
00450
00500
00525
MELong1
Candidatus Mesenet longicola
(may represent two prophages)
BNGT01000027.1
BNGT01000009.1
7140
Assembly Gap
7050
RhuM
6950
RelE
Assembly Gap
3070
Assembly Gap
3230
Patatin
MutL
PLDc
CifB
3290
CifA
O. tsutsugamushi UT144
LAOR01000004.1
0140
0134
0130
0120
O. tsutsugamushi FPW1038
OOHR01000004.1
1274
1266
Transposase
Hypothetical Protein
Truncated / Disrupted
Ankyrin
Prophage WO Homology
Recombinase
Replication & Repair
Connector/ Baseplate
Head
WO-PC1
Tail fiber
Tail
b
Wolbachia WO-like Islands featuring Tail and Lysis genes
WOAlbB2
05905
05850
05815
Ankyrin
WONo4
WOMau3
10070
10100
10150
10200
10250
EAM genes
10350
02985
02910
02935
02960
02985
Patatin
03060

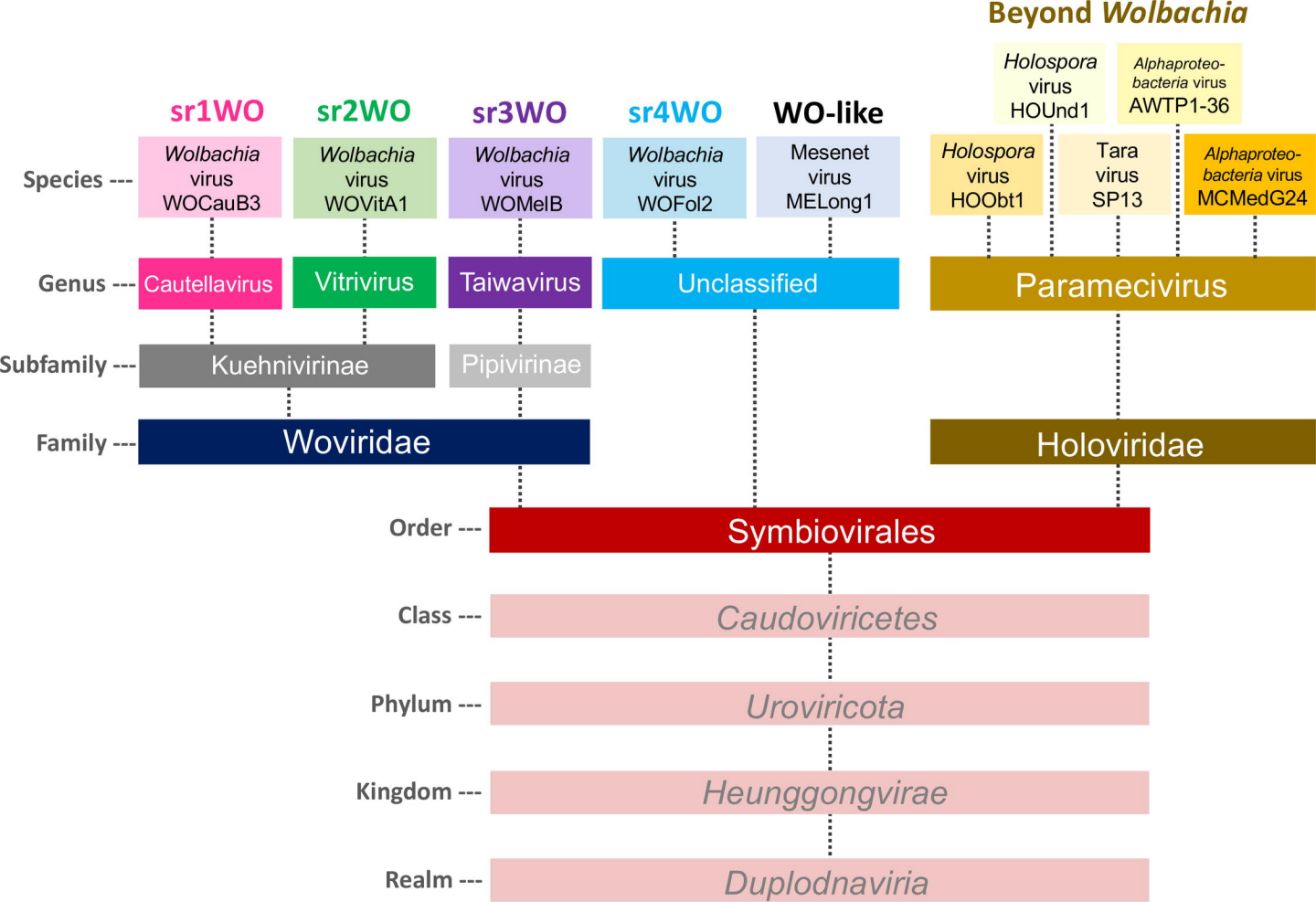
Beyond Wolbachia
sr1WO
sr2WO
sr3WO
sr4WO
WO-like
Holospora virus HOUnd1
Alphaproteo-bacteria virus AWTP1-36
Species ---
Wolbachia virus WOCauB3
Wolbachia virus WOVitA1
Wolbachia virus WOMelB
Wolbachia virus WOFol2
Mesenet virus MELong1
Holospora virus HOObt1
Tara virus SP13
Alphaproteo-bacteria virus MCMedG24
Genus ---
Cautellavirus
Vitrivirus
Taiwavirus
Unclassified
Paramecivirus
Subfamily ---
Kuehnivirinae
Pipivirinae
Family ---
Woviridae
Holoviridae
Order ---
Symbiovirales
Class ---
Caudoviricetes
Phylum ---
Uroviricota
Kingdom ---
Heunggongvirae
Realm ---
Duplodnaviria

a

Distinguishing Order Traits	Symbiovirales			
Host: symbiotic bacteria	✓	✓	✓	✓
Core phage modules: recombinase, replication, head, connector/baseplate, tail fiber, contractile tail, lysis	✓	✓	✓	✓
Large serine recombinase (typing gene)	✓	✓	✓	✓
PAAR gene in connector/baseplate module	✓	✓	✓	✓

b

Distinguishing Family Traits	Woviridae	Holoviridae
EAM	✓	Absent
Ankyrin-repeat containing proteins	✓	Absent
HTH_XRE transcriptional regulators	✓	Absent
Putative lysis gene	Patatin	GH108

c

Distinguishing Subfamily Traits	Kuehnivirinae	Pipivirinae
Integrate into distinct *att* sites	✓	----
Location of EAM in prophage genome	3'-prophage genome	Flanking one or both sides

d

Distinguishing Genus Traits	Cautellavirus	Vitrivirus	Taiwavirus	Paramecivirus
Chromosomal integration	Magnesium chelatase gene or Sua5-intergenic region	VNTR-105	Flanked by EAM, mobile elements	Unknown
Structural module synteny: baseplate -> head -> replication & repair -> tail	✓	----	----	✓
Structural module synteny: replication & repair -> head -> baseplate -> tail	----	✓	✓	----
Direction of ankyrin adjacent to late control gene (relative to tail/patatin)	Opposite	Same	Same	N/A
WO-PC1	✓	Absent	Some	✓
ParB	Absent	✓	✓	✓
Transcriptional regulators (HTH_XRE)	1-domain	2-domain	2-domain	Absent
Undecim Cluster	Absent	Absent	Some	Absent
CifA;B	Some	Absent	Some	Absent
MutL	Absent	✓	Some	Absent